Available online at www.sciencedirect.com
ScienceDirect
Tectonophysics 453 (2008) 122–147
TECTONOPHYSICS
www.elsevier.com/locate/tecto

Seismic deformation in the St. Simeon Monasteries (Qal'at Sim'an), Northwestern Syria

A.S. Karakhanian [a,*], V.G. Trifonov [b], T.P. Ivanova [c], A. Avagyan [a], M. Rukieh [d], H. Minini [d], A.E. Dodonov [b], D.M. Bachmanov [b]

[a] Georisk Scientific Research Company, 24a Marshal Bagramyan, Yerevan, 37019, Armenia
[b] Geological Institute of the Russian Academy of Sciences (RAS), 7 Pyzhevsky, Moscow, 119017, Russia
[c] Institute of Dynamics of Geospheres of the RAS, Block 6, 38 Leninsky Ave., Moscow 117334, Russia
[d] General Organization of Remote Sensing, P.O. Box 12586, Damascus, Syria

Received 2 October 2006; accepted 19 March 2007
Available online 6 February 2008

Abstract

The St. Simeon Fault is 80 km long and stretches from the eastern side of the Al Ghab Depression to the north–east; it links the structures of the Levant and East-Anatolian active zones. Left-lateral strike-slip displacements and deformations of landforms cut by the fault have been recorded. The Sim'an Ridge is located between two branches of the fault and displaced by 1.2 km, overlapping a young depression. As the terminations of these branches at the site of their overlapping converge northerly, the mechanism of structural scissors considerably enhances the lateral extrusion of the Sim'an Ridge. The St. Simeon Monastery, built by the Byzantine in the 5th century AD, is situated on the top of the Sim'an Ridge.

The main church of the St. Simeon Monastery has a cruciform shape, and its eastern wing is deflected by 3–9° to the north. The existing *architectural* explanation of this phenomenon assumes initial designing of this bend by the builders and contains many contradictions. Upon our study of active faults, specific features and traces of seismic impacts on the monastery structures, we suggest an alternative, *seismic* explanation. Our scenario interprets the curvatures of the monastery structures as a consequence of distributed co-seismic or post-seismic deformations in the intra-fault block delimited by the branches of the St. Simeon Fault.

Keywords: Active fault; Archaeoseismicity; St. Simeon Monastery; Monument rotation

1. Introduction

Palaeo- and archaeo-seismological methods to study the surface rupture displacements are well known and parameters of such displacements are widely used in seismic hazard assessments. In the meantime, diffuse deformations within active fault wings and intra-fault blocks are much less studied and rarely applied for the same purpose. Many papers report on the offsets of historical structures and archaeological monuments caused by surface ruptures in the Mediterranean basin (Ellenblum et al., 1998; Nur and Cline, 2000; Galli and Galadini, 2001; Altunel et al., 2003; Meghraoui et al., 2003; Altunel et al., 2005; Marco et al., 2005). Investigations of earthquake-induced deformations of bending and rotation of entire historical structures or their parts are much fewer (Berberian, 1976; Yegian and Ghahraman, 1992; Bottari, 2003).

The aim of this article is *i)* to consider geometry and kinematics features associated with the St. Simeon Fault, which is located at the junction of the Levant Zone (Dead Sea Transform) and the East-Anatolian Fault Zone (EAFZ), and *ii)* to demonstrate the possible seismic origin of the deformations observed in the Monastery of St. Simeon the Stylist (Qal'at Sim'an). The evidence presented in this article was collected during broader archaeo-seismological and geodynamic investigations carried out in Syria in 2005–2006, which included the analysis of remote sensing

* Corresponding author. Fax: +374 1 0 52 23 44.
E-mail address: georisk@sci.am (A.S. Karakhanian).

0040-1951/$ - see front matter © 2008 Elsevier B.V. All rights reserved.
doi:10.1016/j.tecto.2007.03.008

material (Landsat ET, IRS, and *Quick Bird* satellite images), the construction of DEM and large-scale 3D models, the creation of databases in GIS format based on the active fault and archaeoseismicity surveys, as well as geological and archaeo-seismological field works.

2. The active St. Simeon Fault

The active Levant Fault Zone stretching along the eastern Mediterranean coast has a complex structure. It forms the present-day western edge of the Arabian plate and links the Red Sea Rift with the north-western transpressive boundary of the plate that corresponds to the East-Anatolian Fault Zone (Garfunkel and Ben-Abraham, 2001). In the north-western Syria, the Levant Zone is represented by the Al Ghab segment represented by a pull-apart basin (Brew et al., 2001; Rukieh et al., 2005). The system of faults stretching northwards from the Al Ghab Basin links the Levant Fault Zone with the East-Anatolian Fault Zone in the area of the Amik depression (Fig. 1) (Brew et al., 2001; Westaway, 2004; Rukieh et al., 2005).

From the eastern side of the Al Ghab Basin, the 80 km-long St. Simeon Fault branches to the northeast (St. SF in Figs. 1, 2). The St. Simeon Fault is subdivided into two major segments. The southern segment is about 33 km long and runs from the Al

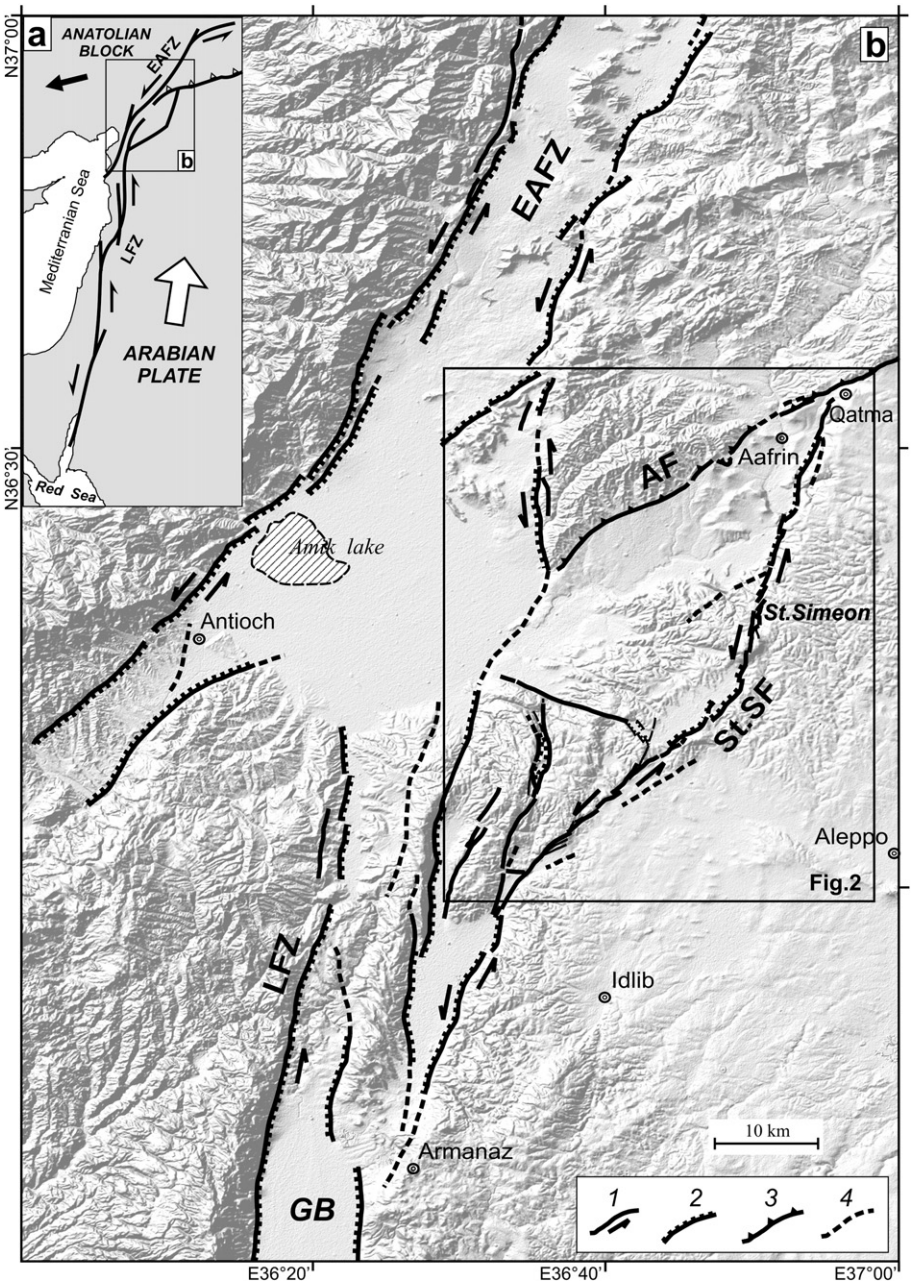

Fig. 1. The St. Simeon Fault in the regional context of junction between the Levant and East-Anatolian Fault Zones. a—overview of the geodynamic framework, b—area of junction between the Levant Fault Zone and the East-Anatolian Fault Zones. 1—strike-slip faults; 2—normal faults; 3—reverse faults; 4—supposed faults. EAFZ—East-Anatolian Fault Zone; LFZ—Levant Fault Zone; GB—Ghab Basin; St. SF—St. Simeon Fault; AF—Afrin Fault.

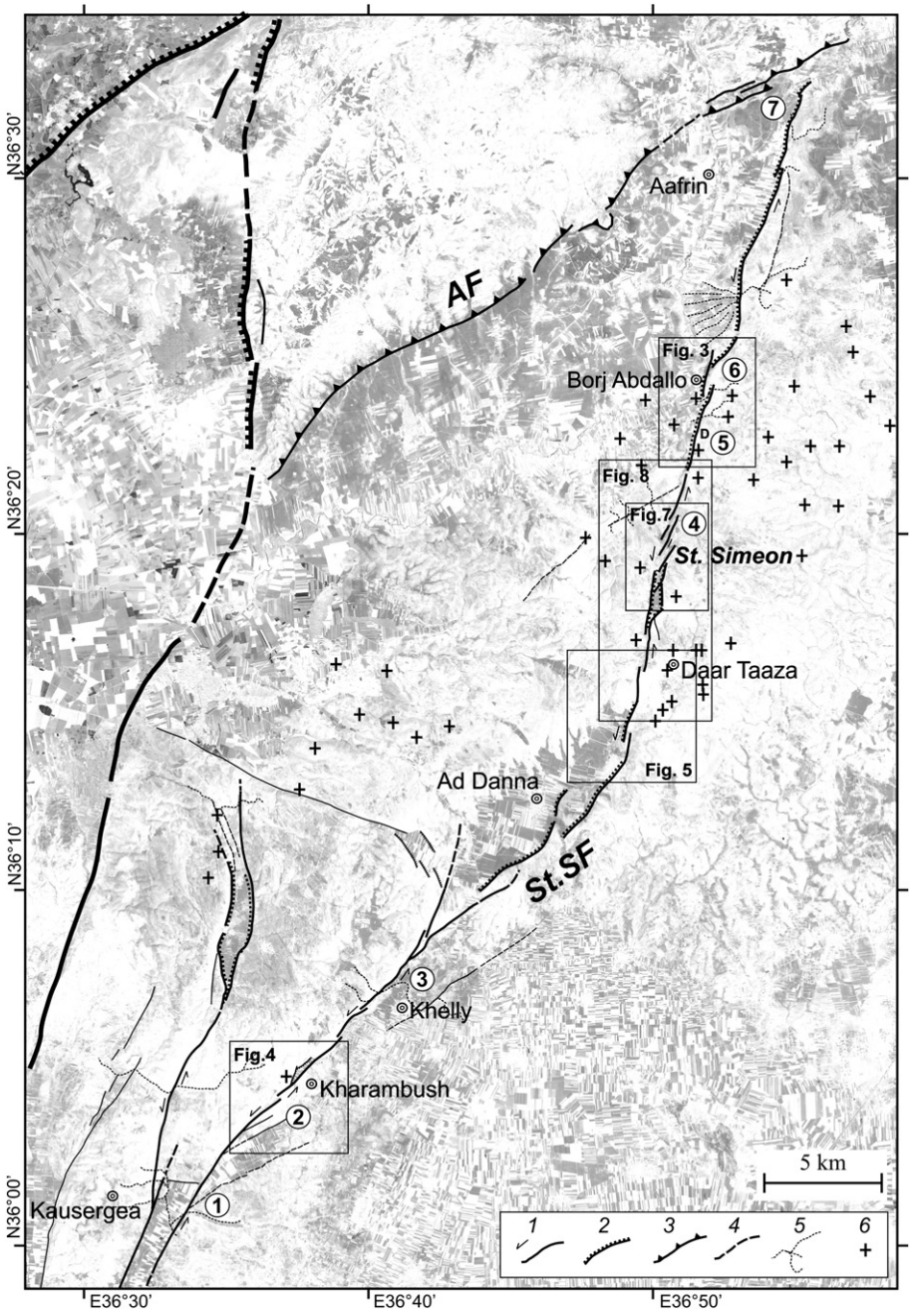

Fig. 2. The St. Simeon Fault. 1—strike-slip faults; 2—normal faults; 3—reverse faults; 4—supposed faults; 5—displaced valleys. 6—*abandoned cities* in the northern karst plateau of Syria (according to Harmanşah, 1999 and the Syria, Archaeology from Space Atlas, 2002); St. SF—St. Simeon Fault; AF—Afrin Fault.

Ghab Basin (the village of Armanaz) to the young depression of Ad Dana. The average strike of this segment is N046° and its eastern wall is downthrown primarily. The northern segment is 47 km long and stretches from the Ad Dana depression to the village of Qatma; the average strike of this segment is N017°. The western wall is downthrown everywhere, except in its southernmost part. Both segments also split into a series of sub-segments with a left-stepping geometry.

The geometry of the Ad Dana depression is similar to a pull-apart basin. The southern, western and eastern sides of this depression correspond to clear normal and strike-slip faults, while the northern side is slightly deformed and gently inclined towards the interior of the depression (Fig. 2). The depression is 14 km long 4 km wide. In the north, the St. Simeon Fault joins the Afrin Fault (AF in Figs. 1, 2), which belongs to the EAFZ. The Afrin Fault mainly developed in the Miocene, but it is still active today (Rukieh et al., 2005). Thus, the St. Simeon Fault takes a boundary position, linking the two lithospheric scale structures of the Levant and East-Anatolian zones (Fig. 1).

From the morphological point of view, the St. Simeon Fault is marked by a topographic scarp up to tens of meters high. Our detailed examination shows that actually this single fault scarp is stepped and subdivided into several minor parallel scarps. The scarp-forming fault branches are steeply inclined (70–90°)

Fig. 3. The St. Simeon Fault near the valley with known Paleolithic caves of Hodedeirieh (Dederiech) I and II (Site 5 in Fig. 2). (A)—(A')—left-lateral strike-slip displacement of the valley thalweg by 250 m. (1) and (2)—the Palaeolithic caves of Hodedeirieh (Dederiech) I and II located directly close to the fault zone.

more often towards the uplifted wall (Sites 2, 4, 5 and 6 in Fig. 2). The vertical displacement component is smaller than the strike-slip one. Striations found on individual discontinuity planes are horizontal, or gently inclined to the north or to the south (4, 5 in Fig. 2). Landforms cut by the fault display regular left-lateral offsets and associated deformational bends. The largest of such structures generated an offset of ~850 m of the Al Num River valley (Site 1 in Fig. 2) and ~1000–1200 m of the Kaini River (Site 3 in Fig. 2).

On the northern segment, the valley known for its Palaeolithic caves—Hodedeirieh (Dederiech) I and II, and the one located near the village of Burj Abdalo, curve to the left by 200–250 m and ~550 m, respectively (Site 5 in Figs. 2, 3). Cemented conglomerates supposedly of a Middle Pleistocene age are preserved on the slopes of the displaced valley in the Burj Abdalo village. To the northeast of the Afrin City, near the village of Arpi-Qibar, another river valley is shifted by ~ 650 m left-laterally (Site 7 in Fig. 2).

Beyond the river valley offsets, deformations of large landforms with a left-lateral kinematics can be observed on both segments of the St. Simeon Fault. The fault cut and shifted individual ridge spurs and valley sectors, and created overlapping structures. A typical structural form of this kind is found near the village of Kharambush (Site 2 in Figs. 2, 4a, b), where a depression (Site B in Fig. 4) is overlapped by a ridge spur cut by the fault (Site C in Fig. 4) suggesting a left-lateral offset of about ~2–2.5 km (points A and A' in Fig. 4).

A similar pattern is observed west of the Dar Taaza village, where the summit of Mount Jebel Sheikh Barakat is offset by ~1.2 km to the left (Fig. 5a, b), generating the overlap of the summit with a narrow part of the valley near the village of Fahoura. In earlier works, Ponikarov et al. (1967) the offset of the summit was estimated 600 m.

On the northern segment of the fault, 1 km east of the Gazzavia Village (Site 5 in Fig. 2), we studied a small quarry in the Quaternary alluvial fan of a small river, on the eastern bank of the Saint Simeon-Afrin motor road (N36°22′38.8″ E36°51′ 23.1″). A clear reverse fault with its plane striking N30° is recorded in the northern wall of this quarry. The Quaternary conglomerate, containing two palaeo-soil horizons is displaced by this reverse fault by 1.5 m (Fig. 6). Several meters farther, an antithetic normal fault with a displacement of 0.5 m was recorded in the uplifted wall of the reverse fault. The scarp of the main fault is located at a distance of 400–500 m to the east of the quarry. It is likely that the reverse fault motion recorded in the quarry is due to a deviation of the local fault strike azimuth by 15–20° to the east (from the general strike of N17°) eventually causing an increase of compressional component.

The site near the village of Deir Sim'an and the Qal'at Sim'an monastery/fortress (Fig. 7) is crucial for the study of the displacement along the St. Simeon Fault. The monastery and the surrounding fortress were built on a small ridge consisting of Helvetian and Tortonian limestone and limestone breccias (Geological Map of Syria, 1964). The Sim'an Ridge is 1.7 km long and 0.2 to 0.5 km wide. The ridge is asymmetric: its eastern side is steep and the western one is gently sloping (Fig. 7). The Sim'an Ridge is located between the terminations of the two sub-segments of the St. Simeon Fault (indicated S and N in Fig. 8) arranged with left-stepping geometry. Young tectonic depressions (D1 and D2 in Figs. 7, 8) formed outside the limits of the Sim'an Ridge, on the downthrown sides of both sub-segments. On the southern sub-segment (S), the western side is uplifted and the fault plane is inclined to the east, while on the northern (N) one the situation is specular (Figs. 7, 8). Directly at the site of the Sim'an Ridge, the planes of these sub-segments curve helicoidally and gain a dip oriented reversely, opposite to the slope. Along with this, the strike of the southern sub-segment changes sharply, from N0° to N33°. Northeast of the monastery, the southern sub-segment changes its strike to N16°,

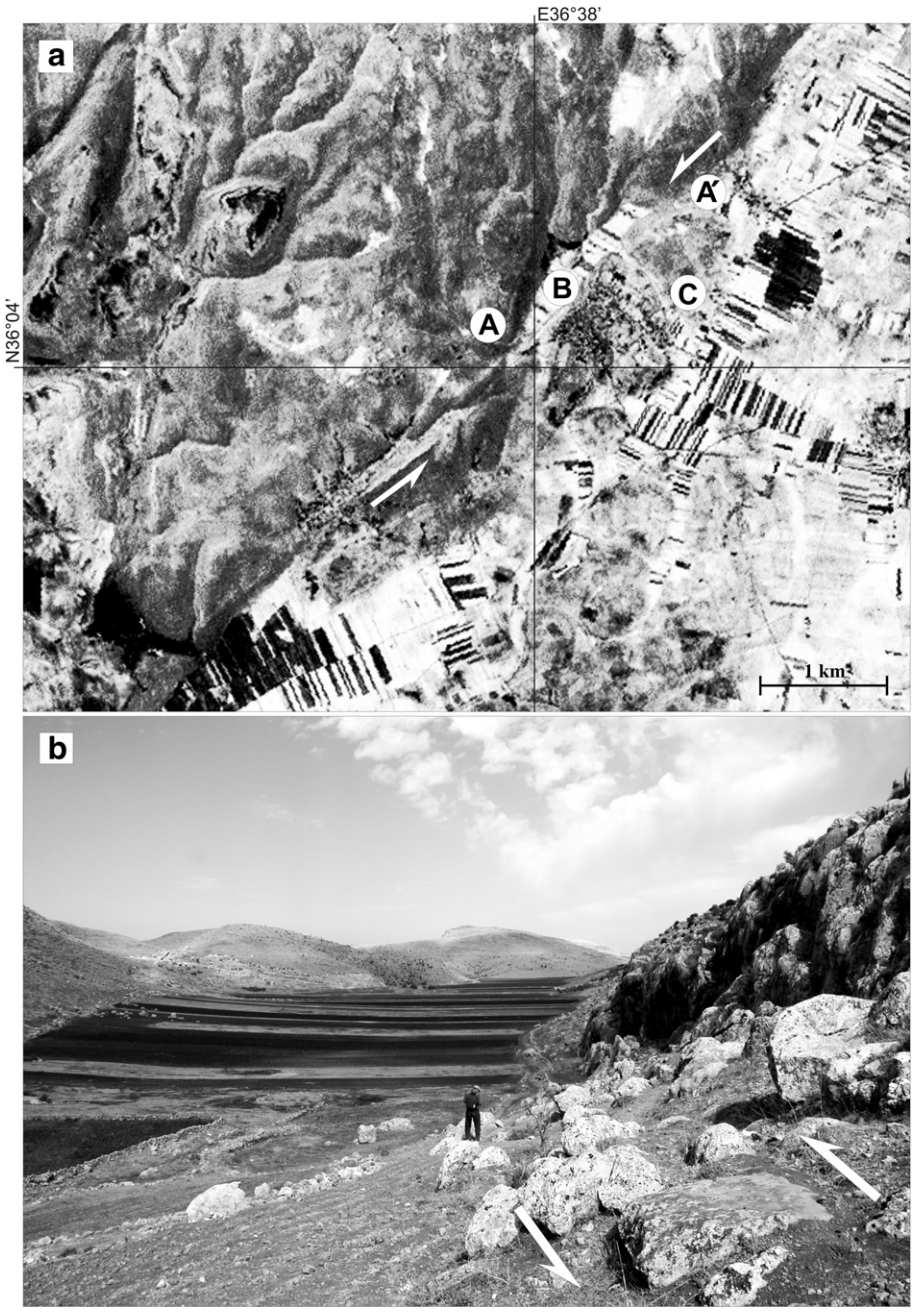

Fig. 4. a—The St. Simeon Fault near the village of Kharambush (Site 2 in Fig. 2). The dislocated part of depression (B) is overlapped by the ridge spur cut off by the fault (C), and points (A) and (A′) indicate the amount of left-lateral displacement corresponding to ~2–2.5 km. b—field photo of the valley B taken from Site A in Fig. 4a.

continues to the north and joins the northern sub-segment (Figs. 8, 9 and 10). By restoring its initial strike, the fault plane of the southern sub-segment experiences a helicoidal distortion and regains the western dip. Thus, a fault scarp >2 m high can be observed at a distance of 100 m from the northeastern corner of the fortress wall (Site D in Fig. 9) oriented N25° and dipping 77°–85° W. The sliding furrows are horizontal, or inclined to the south. Two systems can be distinguished in the extension cracks and fragmentation related to this fault: in one system, cracks are oriented NNW (345–355°) and dip W70°–85°, while the other cracks are sub-latitudinal., with dip angles of N75°–85°. Fragmentation zones in the first and second systems of cracks are up to 20 cm and 30 cm thick, respectively. On the western slope and near the crest of the Sim'an Ridge, there are minor scarps located with *en echelon* geometry and bearing unclear horizontal striation (Sites A, B and C in Figs. 9; 10b, *c*). Part of them can represent secondary fractures and breaks formed during motions along the principal faults. In the meantime, as far as it was possible to establish, the scarp planes dip steeply to the east, opposite to the slope (Figs. 9 and 10).

The obtained pattern allows us to suggest that the Sim'an Ridge represents a fault bridge (shutter ridge) between the two young depressions—D1 and D2 (Figs. 7, 8 and 9). Left-lateral strike-slip displacements along the southern sub-segment have

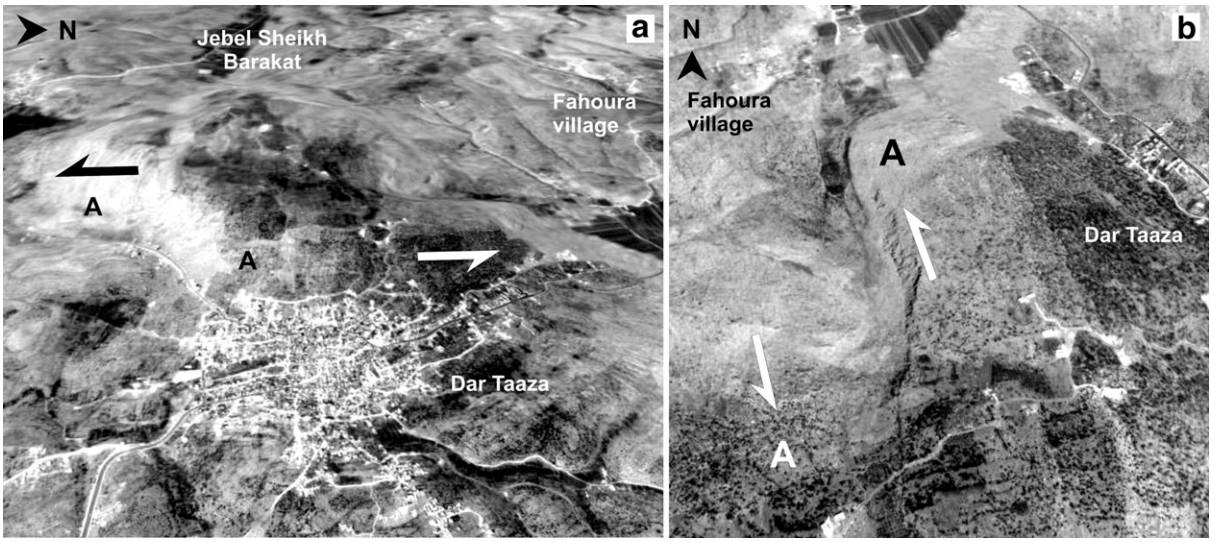

Fig. 5. 3D model of Mt. Jebel Sheikh Barakat prepared using DEM 3^{I} and *Quick Bird* satellite image with the resolution capacity of 0.6 m. Points A–A^{I} emphasize 1.2 km of left-lateral strike-slip offsets along the St. Simeon Fault. a—view to the Mount Jebel Sheikh Barakat from the east; b—a view of the Mount Jebel Sheikh Barakat from the south.

led to the lateral protrusion of the Sim'an Ridge in the southwestern direction and the overlap between the young depressions (Figs. 8 and 9), like the one observed near the village of Kharambush and the summit of Jebel Sheikh Barakat. The left-lateral motion of the Sim'an Ridge amounts to 1 to 1.2 km, which is well comparable with similar displacements estimated for the summit of Jebel Sheikh Barakat and the Kaini River.

Considering that the sub-segment terminations at the site of their overlap near the Sim'an Ridge converge northwards, the oblique pushing of the Sim'an Ridge toward the southwest can be strongly amplified by the mechanism of *structural scissors* as shown in Fig. 9b.

A similar picture was observed 5 km north of the Sim'an Ridge, in the quarry wall (Fig. 6). This increasing compression in combination with lateral pushing can lead to transpression and, as a consequence, produce secondary scarps and cracks forming *flower*-type structures near the top of the Sim'an Ridge (Sites A, B and C in Figs. 9; 10*b, c*).

Apparently, the seismic history of the St. Simeon Fault was rich in events, but it has been studied insufficiently. Important studies of archeoseismicity were conducted in the Al Ghab Basin (Syria) and near Lake Amik (S. Turkey) by Sbeinati et al. (2005), Meghraoui et al. (2003) and Altunel et al. (2005), but they did not consider the St. Simeon Fault. Accounts contained

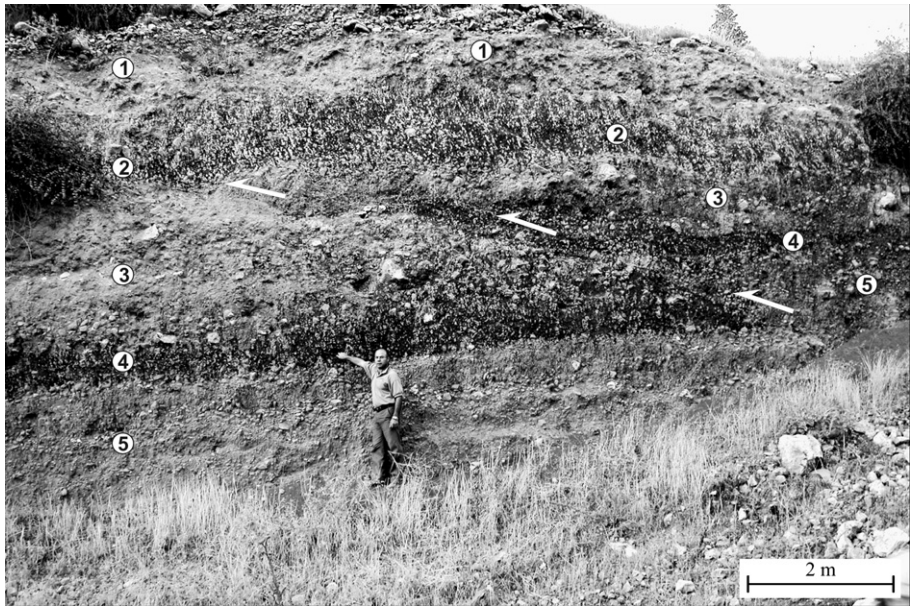

Fig. 6. The reverse fault with displacement amplitude of 1.5 m in the quarry wall, 1 km east of the Gazzavia village (Site 5 in Fig. 2): 1—soil not displaced by the ruptures; 2—dark loams and loamy sand; 3—loam with colluvium debris; 4—dark loam and loamy sand with thin layers of marl and gravel; 5—pebblestone with loamy sand in the base.

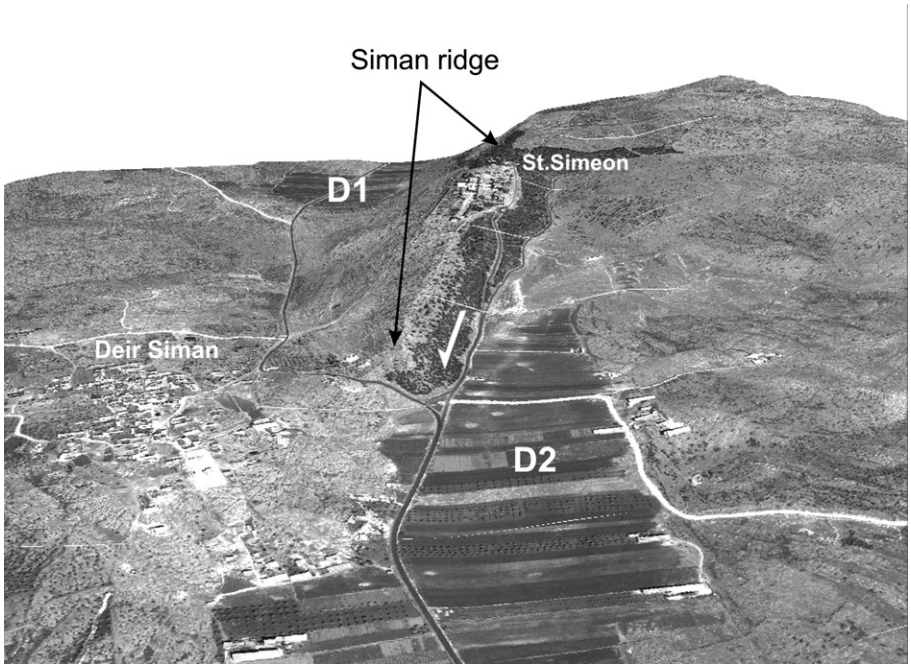

Fig. 7. 3D-model of the Sim'an Ridge created using a DEM and Quick Bird satellite image with resolution capacity of 0.6 m. The horizontal to vertical scale ratio is 1/1.5.

in historical chronicles primarily describe strong earthquake damages in the cities of Aleppo and Antioch and do not provide any direct evidence of seismic activity in the region of the St. Simeon Fault. In the meantime, our observations show that the mentioned break in the quarry wall (Fig. 6) alone could attest to at least two episodes of strong paleoseismicity along the St. Simeon Fault Zone.

Another manifestation of the recent fault activity can be associated with the collapse of a man-made grotto built in a scarp on the eastern fault side, near the village of Kharambush (Fig. 4). The cultural layer buried under the collapsed roof of that grotto incorporates antique and Early Byzantine ceramics and utensils.

The *abandoned cities* in the north of Syria can provide abundant and unique information about the historical seismicity. In the 3rd–4th centuries AD, rapid growth of population in Northern Syria led to the agricultural development of barren lands on the karst plateau in the north of Syria and within the areas of Haran and Jebel al-Arab in the south (Harmanşah, 1999). More than 700 medium-scale and minor settlements appeared on the limestone hills of the karst plateau—mostly small towns with good street planning, houses and Byzantine churches built of large regular blocks of limestone extracted locally. The second half of the 6th and the early 7th centuries were marked by the decline of these settlements following land degradation, strong earthquakes and the Islamic expansion (Harmanşah, 1999). Such towns saturate the region of the northern segment of the St. Simeon Fault (Fig. 2). Today, most of these are *dead* or *ghost* cities, which are nevertheless well preserved. The unique rate of preservation, along with features of the area and landscape planning in these settlements, have raised considerable interest among archeologists, historians and architects for a long time. Presently, a project on establishing an Archaeological Park in this area is developed.

In the meantime, these abandoned towns are of inestimable importance for seismic hazard assessment and study of local seismic culture, since they bear numerous traces of repeated impacts of strong seismicity and human attempts to withstand the destructive force of earthquakes. In this regard, the town of Deir Sim'an (Telanissos) and the monastery fortress of St. Simeon (Qal'at Sim'an) are among the most important structures of this kind.

3. Architecture and history of the St. Simeon Monastery (Qal'at Sim'an)

The cathedral of St. Simeon was constructed in 476–490. The cruciform shape was achieved through an original combination of architectural design elements practiced at that time. The octagon with the sacred pillar, where saint Simeon the Stylite (392–459 AD) preached for more than 40 years, an analog of atrium, was placed in the centre and, supposedly, covered by a wooden roof (A in Figs. 11; 16 and 17). Four wings, each in the form of 3-nave basilica, were connected to it in the form of a crucifix (Butler, 1920). The northern, southern and western wings were almost squared (25 × 24 m), while the eastern wall was longer, up to ~32 m, and had three apses on its termination. The walls of the cathedral were built of local limestone blocks. The foundation of the walls was hollowed in the bedrock limestone to a height of up to ~1 m. In contrast, the western wing stood on the bedrock near to the octagon only, but westerly it rested on the arched colonnade forming a loggia (B in Fig. 11). The basement of the sacred pillar has a square section and was likewise hollowed in the hard rock. The

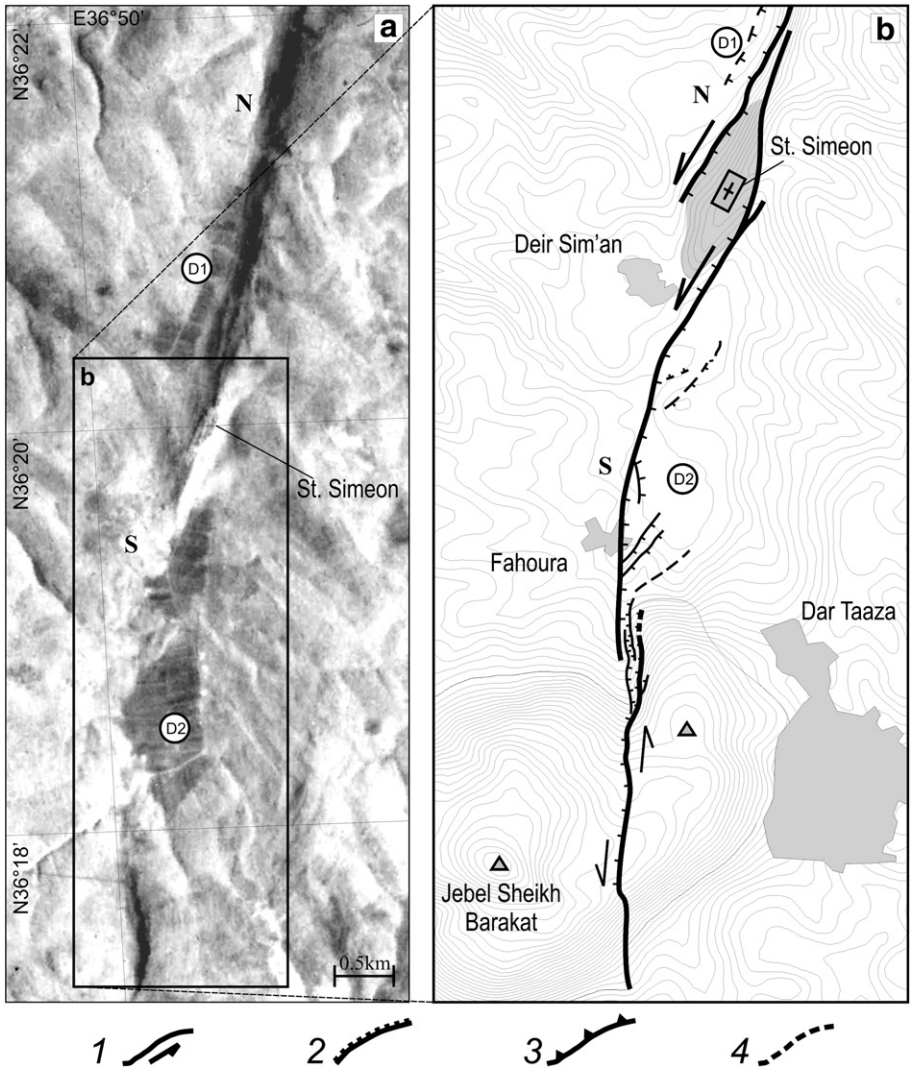

Fig. 8. The St. Simeon Fault near the St. Simeon Monastery. a—satellite image with 10 m resolution capacity, b—interpretation of fault geometry by the data of remote sensing and field works. S—the southern sub-segment; N—the northern sub-segment; 1D and 2D—young depressions. 1—strike-slip faults; 2—normal faults; 3—reverse faults; 4—inferred faults.

western, northern and southern wings of the church hosted the faithful and pilgrims, the eastern one was used for service and the central octagon with the pillar was a memorial place. Originally, the entrance to the church was located in the western wing, but early in the 6th century it was moved to the southern wing.

In late 5th–early 6th centuries, after the main church was built, a number of other buildings rose near it and turned the place to a monastery (Tchalenko, 1953). The most important of these buildings (listed from the north to the south) were the chapel (C in Fig. 11; C in Fig. 17) close to the eastern wing, the Convent—a dormitory for monks, the Baptistery with a small chapel adjoined to it (D, E, and F in Fig. 11), and an entrance to the lower terrace (H in Fig. 11).

According to Tchalenko (1953), seven stages of construction of various parts of the monastery can be distinguished within the period of 475 to 560. Most researchers agree that the main church was built within 476–490 and the octagonal memoral and all four wings of the main church were being built concurrently. However, Ecochard (1936) suggests that the octagon was built first, as a memorial monument, and only later the four arms of the main church were added to it. The Baptistery was also built in 476–490, but after the main church had been completed. The chapels adjoining the main church and the Baptistery were erected in late 5th–early 6th centuries, and then followed the construction of the Convent buildings.

The monastery suffered great damage during one or several strong earthquakes in the first quarter of the 6th century. Apparently, the main church lost the dome above the central octagon at that time (Krenker, 1939), despite Ecochard (1936) thinks this could have happened even at the stage of construction. In any case, Evagrius, who visited St. Simon in 560 AD, saw the central octagon and described it as an atrium (Tchalenko, 1953).

Tchalenko (1953) suggests that late in the 6th century the monastery was reconstructed, but then again destroyed by

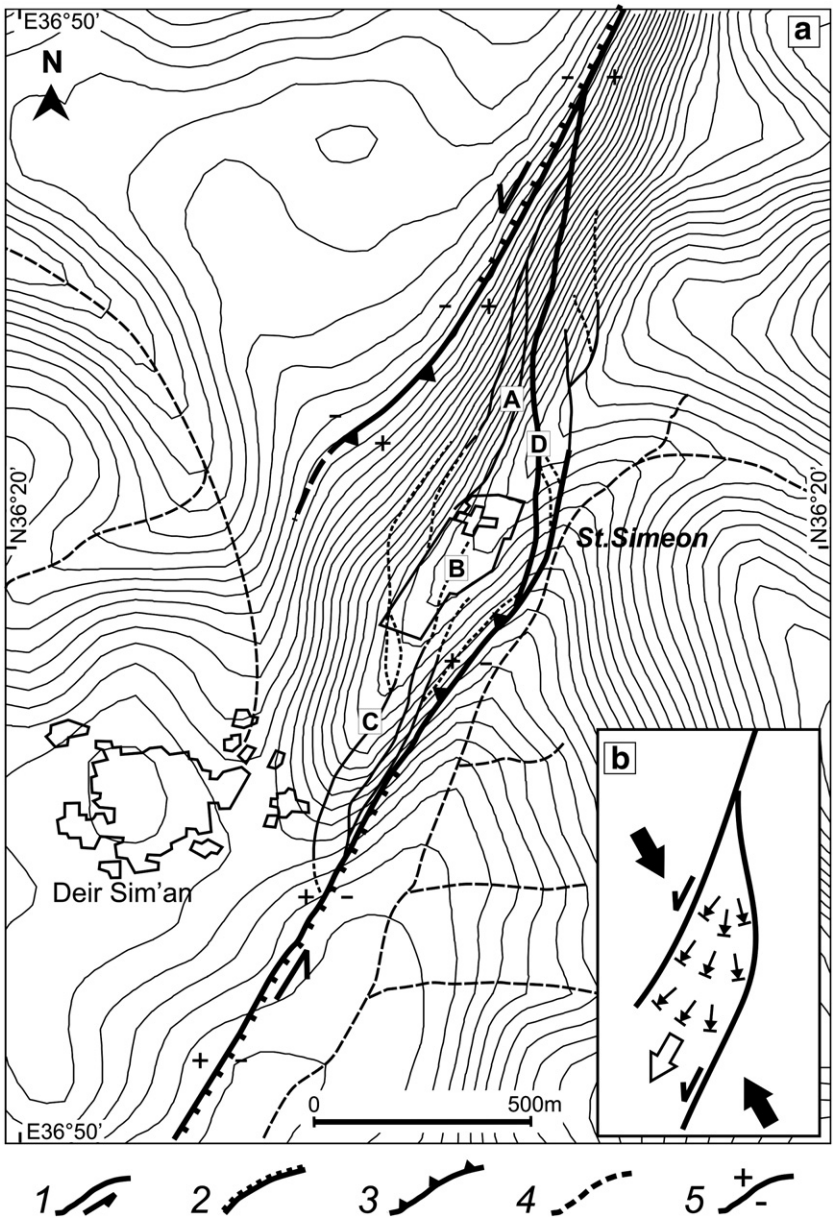

Fig. 9. Active faults in the region of the Sim'an Ridge. a—interpretation based on the remote sensing data and field works; b—the conceptual model.

Arabic invasions in the 7th century. By the time Byzantium regained its control of this area in the 10th century, the greater part of the main church had been destroyed and the eastern wing basilica had been used for service only (after being restored and rebuilt). The mosaic floor in the basilica and, possibly, parts of its walls were reconstructed during the reign of Emperor Basil II (976–1026) and his brother Emperor Constantine VIII (976–1028). Some records are available for these activities that started probably in 979 and were completed in 986. An inscription from this period commemorates works of restoration in the church, as well as the elaborate mosaic pavement (Tchalenko, 1953). In the same period, the monastery was surrounded with a strong fortification wall with towers and was transformed into a fortress (which gave it the present-day name of Qal'at Sim'an—the Fortress of St. Simeon). In the 11th century, the fortress was conquered by the Arabs and the monastery ceased its activity after 1017. It suffered during the conquest and later from the earthquakes, was abandoned and deserted. However, as late as in the 16th century, the eastern wing of the main church and the Baptistery were still used by local population for housing. Today, the monastery and the fortress are a museum.

4. Seismic destruction and deformation

4.1. Telanissos (Deir Sima'an)

There are many traces of seismic impacts in the well-preserved ruins of the Byzantine town of Telanissos that is now located in the area of the modern village of Deir Sima'an (Figs. 7 and 8), 1 km west of the Qal'at Sim'an. Numerous rotations of stone blocks, primarily anti-clockwise, as well as translational dislocations of blocks in the south–southwestern direction are very characteristic

Fig. 10. Photos of fault scarps on the slopes and the crest of the Sim'an Ridge. a—the northern sub-segment is shown by white arrows, and the southern one by black arrows. b—fault scarp on the western slope of the Sim'an Ridge (point B in Fig. 9); c—supposed fault scarp in the area of the St. Simeon Monastery (point C in Fig. 9).

features of these impacts (Fig. 12g, h, i, j, k and l). Some cases of S-shaped seismic deformation of walls are recorded as well. A noteworthy feature is that many of the buildings were built with earthquake engineering design elements (Fig. 13).

Apparently, the town was ruined by the same seismic events that destroyed the St. Simeon Monastery. However, our preliminary inspection did not allow us to record any signs of restoration or reconstruction of the buildings in the period of the 6th–10th

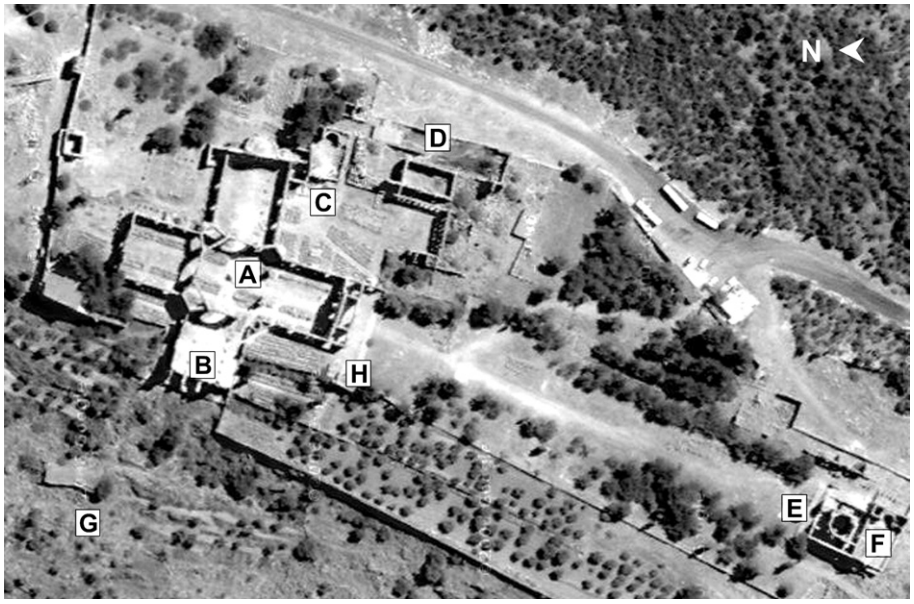

Fig. 11. The *Quick Bird* satellite image for the area of the St. Simeon Monastery: A—main church; B—the western wing (loggia); C—the main church chapel; D—the Convent; E—the Baptistery; F—the Baptistery chapel; G—a *bastion*, or water reservoir; H—entrance to the lower terrace.

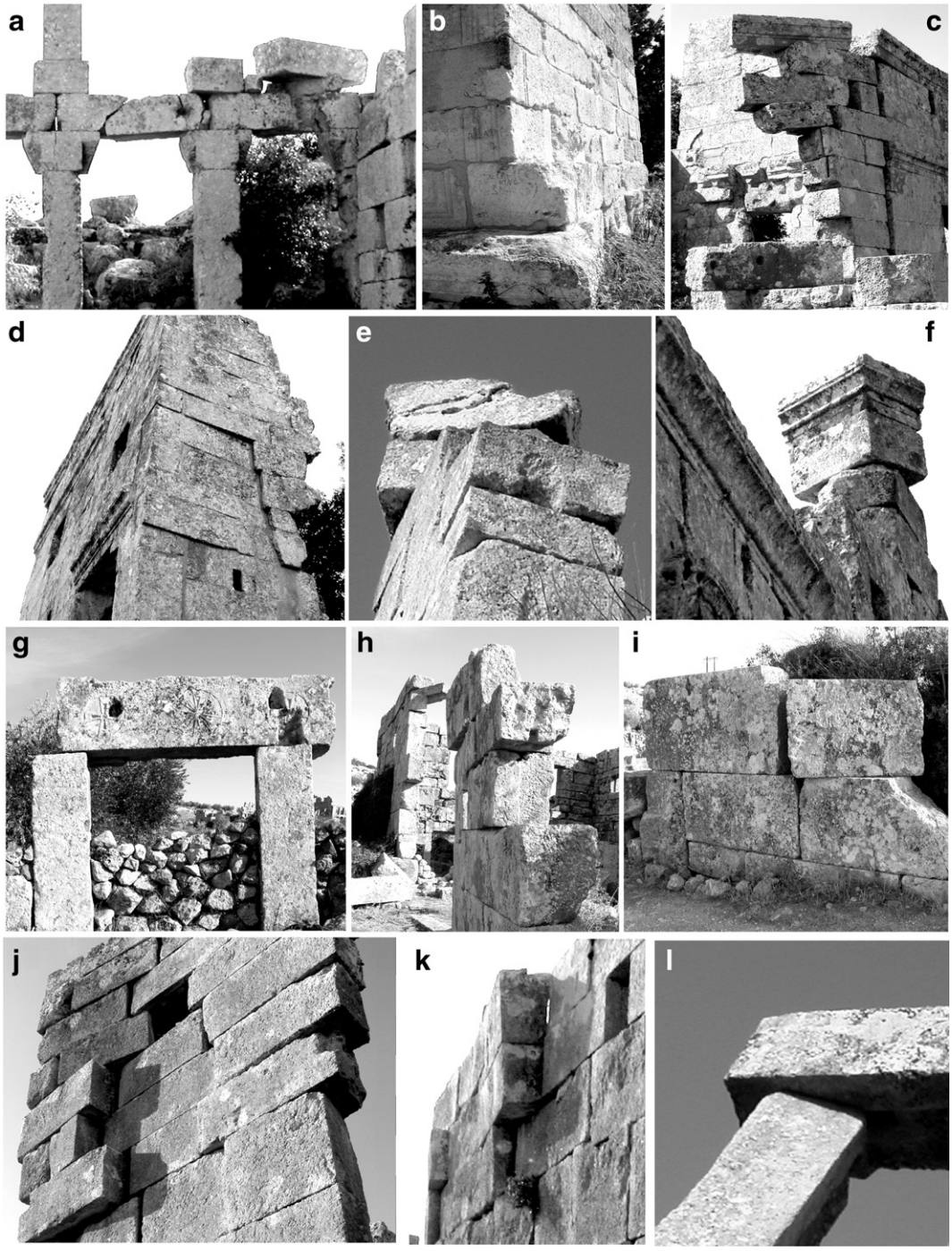

Fig. 12. Effects caused by seismic destruction of buildings and block rotations in Telanissos and the St. Simeon Monastery (*a, b, c, d, e and f*—St. Simeon; *g, h, i, j, k, l*—Telanissos).

centuries. The rare evidence of re-occupation of the buildings, judging from the implementation technique, must be related either to the Middle Ages, or to the modern era.

4.2. St. Simon (Qal'at Sim'an)

Extensive damage of roofs, collapsed columns, strong destruction of walls of the monastery buildings and fortress structures are recorded throughout the Qal'at Sim'an area. Seismic destruction is greater and more important in the western and eastern wings of the main church, while the northern and southern wings are less damaged. Rotations of rectangular stone blocks or even entire masonry layers are recorded in the main church, the Baptistery and other structures. Individual rotation angles are 90–100° (Fig. 12e, f). Indications of strong seismic effects are revealed also in other monastery structures, including those used at the late stages of its activity (the 10th–11th centuries), and within the fortification walls. The outer

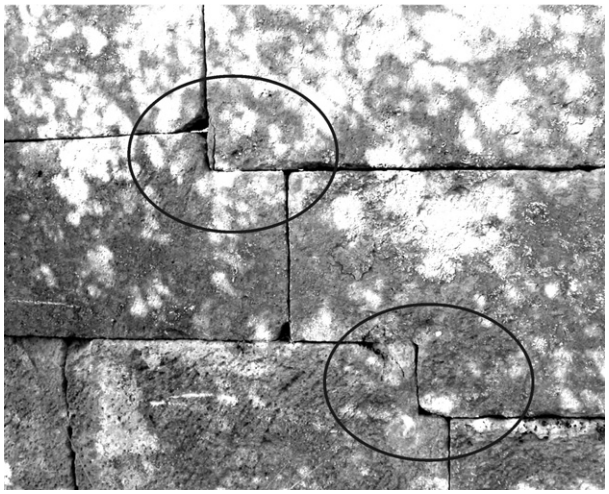

Fig. 13. An example of earthquake engineering design elements in Telanissos.

(western) part of the loggia resting on the arcade is destroyed almost completely. The arcade itself was damaged as well, which necessitated placing support pillars of column fragments and stone blocks beneath it. Individual wall fragments incorporate stone blocks of different size and quality, which is apparently a result of restoration activities. Together, these observations suggest several strong earthquakes and at least two, or even three, stages of restoration after seismic destruction within the period of activity in the monastery/fortress (the 6th–11th centuries).

We have not succeeded in finding any evidence of displacements along surface ruptures in the area or structures of Qal'at Sim'an located within the tectonically stressed block between the two segments of the St. Simeon Fault. Neither was it possible to trace clearly the fault scarp across the fortress walls and monastery structures. Possibly, the scarps were evened during construction and then covered by the cultural layer.

However, 80 m north of the present-day entrance to the monastery, a part of the western fortress wall is strongly damaged. The fortress wall consists of two clearly detectable generations—the lower ancient and the upper younger sections (A and B in Fig. 14). The lower and older parts of the wall was broken through by a large vertical crack along which the wall protruded by 0.7 m to the southeast (Fig. 14). Later, the crack was sealed and new rows of stone were added at the top of the wall. The chronicle sources allow us to suggest that the fortress wall reconstruction must be most probably related to the end of the 10th century AD. Visual inspection does not enable us to determine whether this crack and the displacement by 0.7 m resulted from the damage the siege could cause to the wall, or appeared as a consequence of ground shaking generated by a strong earthquake or even displacements along one of the secondary surface ruptures.

We recorded regular bends in the main church structures, both chapels and some auxiliary buildings that can be interpreted as the effects of distributed deformations associated with fault motions. To assess the character and the amount of such deformations, we performed field measurements of individual monastery structures and determined the orientation of walls. The accuracy of our measurements did not exceed ±1°. Therefore, structural distortions by <2° were not accounted for. The obtained data along with detailed architectural layouts, *Quick Bird* satellite images (with a resolution of 0.6 m) and air

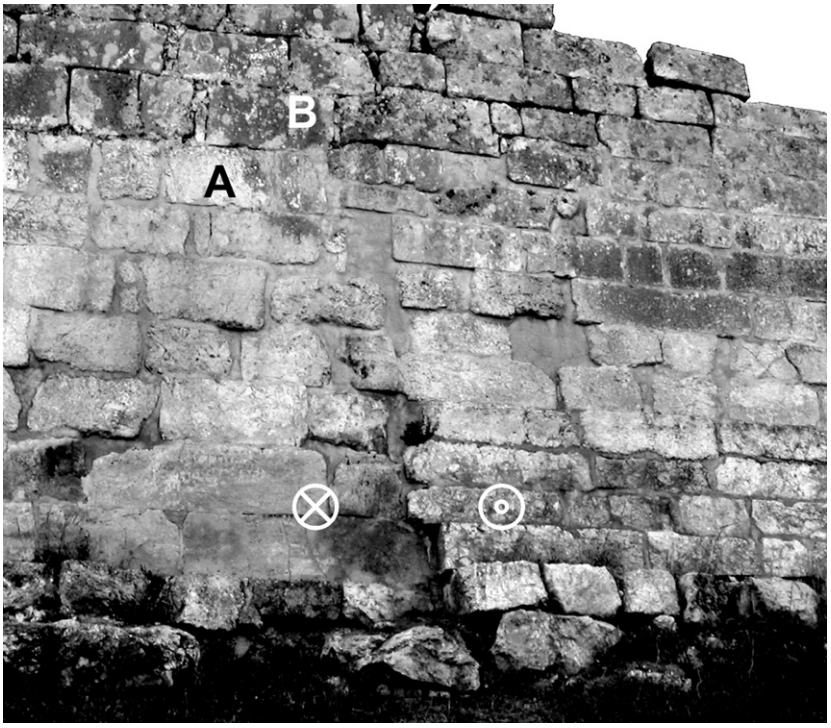

Fig. 14. Vertical crack and displacement of the western fortress wall foundation by 0.7 m. A—the old generation of walls; B—the younger generation of walls.

photographs composed the database, which was later analyzed in *ArcGIS 9.1* to build 3D models using the *Arc Scene* modules.

For a long time, the main cathedral of the St. Simeon Monastery has attracted the attention of architects and archeologists by its architectural paradox: its eastern wing is declined to the north from the position it would need to have in the true cruciform design (Butler, 1920; Krenker, 1939; Tchalenko, 1953).

Our field inspection showed that the walls of loggia located in the western wing of the main church are also bent northwards and bear evident traces of seismic deformation (Site B in Fig. 11). This deformation is most clear on the south-western termination of the loggia that has not been touched by recent restorations. The wall basement preserved in this place could have earlier supported a part of loggia that did not survive, or could be a part of the original entrance structure. Presently, the row remaining from this wall farther serves as a retaining wall for the southern monastery terrace. This wall is indicated in Fig. 15a. The masonry of the preserved wall basement is similar to the masonry in the loggia and the western wing and consists of three rows of hewn stones, meanwhile the rest of the terrace-retaining wall has a drastically different masonry only one-stone wide (Fig. 15a).

The wall direction in the western wing of the main church is N100°. However, at the site shown in Fig. 15a the strike changes to the azimuth of N95°, and farther to N106°, thus creating a small arc-shaped bend of the wall accompanied by considerable northward dislocation of its end part. The termination of the wall is bent by 9° clockwise, which, given that the deformed wall portion is 16 m long, determines the bend amplitude of 3 m. The opposite, north-western flank of the loggia wall is located 23 m to the north (C in Fig. 15c) and is

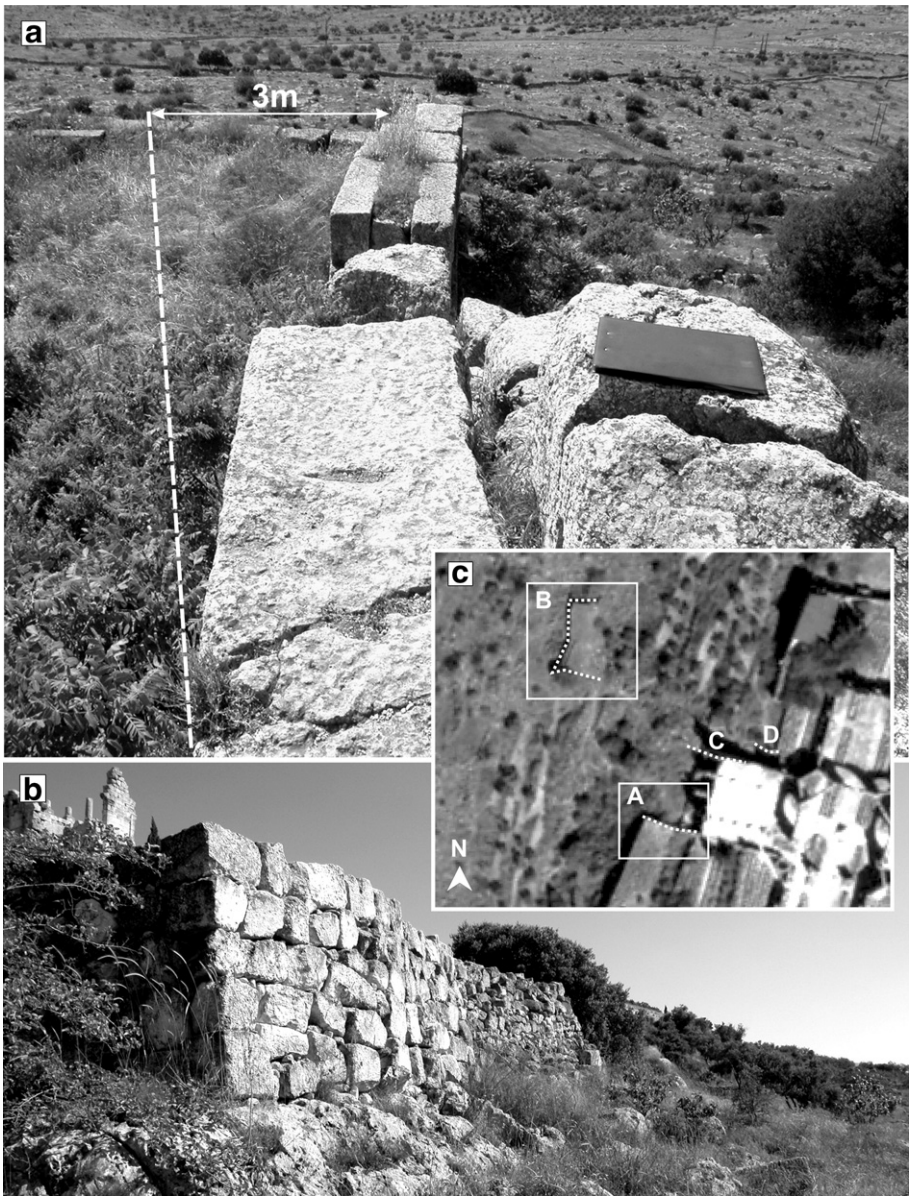

Fig. 15. Earthquake-induced bending deformations on the western wing in the St. Simeon main church. a—wall curve; b—curve of the frontal wall and the southwestern corner of the *bastion*; c—Quick Bird satellite image for the western wing area (A, C and D—curves of different walls in the loggia, B—the *bastion*).

also bent 8° clockwise with a resulting offset of 1 m. Another distortion is recorded 4.5 m farther to the north, where a fragment of the retaining wall is bent by 7° in the same direction and deflected by 0.5 m (D in Fig. 15c).

Considerable curves are revealed in the walls of a small structure situated 50 m west of the loggia, down by the ridge slope (B in Fig. 15c; b). It has an irregular quadrangle layout and could correspond to a reservoir basin or a destroyed bastion. The greatest distortions are recorded in the south-western corner of this structure, showing signs of later, post-Byzantine restoration. At this place, a part of the western wall is slightly bent northwards as a result of a clockwise twist (Fig. 15b). A sharper counter-clockwise turn is noticed in the westernmost section of the southern wall. Unfortunately, considerable reconstruction of this structure does not allow us to give any certain estimate of the amount of displacement and the time of the deformation.

As mentioned above, the eastern wing is bent northwards and turned counter-clockwise with respect to the other three wings of the Cathedral (Fig. 16). The axis of symmetry drawn in the east–west direction through the center of the western wing to the octagon center to the pillar is oriented N100° (Figs. 16 and 17). If the church wings departed from the center at right angles, then the eastern wing, like the western one, would have had an azimuth of N100°. However, the strike of the eastern wing measured along its central axis, i.e., from the pillar to the altar and main apse center, is N97° (Figs. 16 and 17). This derives the estimated angle of deflection of the eastern wing by 3° from the cruciform orientation as recorded in the published sources (Butler, 1920; Krenker, 1939; Tchalenko, 1953).

Both walls in the eastern wing are oriented N94° and the same orientation can be measured for the 6 column bases that have remained on the southern side of the wing. Therefore, the deflection of the eastern wing as measured by the walls, columns and floor elements exceeds the value of 3°, reaching 6° (Fig. 17). Curvatures are observed in the wall basements hollowed in the bedrock limestone, and also in block-masonry wall portions. Because of the curvature, the southern wall of the eastern wing is ~3 m longer than the northern one. The longer axes of rectangular stone plates paving the floor in the eastern wing and in the octagon are oriented with the same azimuth of N94°. Some parts of the eastern wing floor are paved with mosaics, which apparently had two periods of creation (Tchalenko, 1953). The older mosaic preserved in the eastern part of this wing has more elaborate floral pattern and can be distinguished from the younger one. The latter is oriented mostly N94° and has less refined, geometric pattern. The stone plates and the geometric mosaics in the eastern wing were laid during the restoration works of the 10th century as indicated in the inscription inserted into the mosaic mentioning the name of Emperor Basil II (Butler, 1920; Krenker, 1939; Tchalenko, 1953).

By the northern and southern sides of the iconostasis and altar area, there are two small rooms named, respectively, *Prothesis* and *Diaconion* (E and C in Fig. 17). The basements of the iconostasis, altar, main apse and *Prothesis* were hollowed up in the bedrock. On their southern and northern sides, walls in the eastern wing join the iconostasis and altar at angles of N93° and N87°. Meanwhile, at the opposite end, angles of junction between the eastern wing walls and the walls of the northern and southern wings correspond to N96° on the southern side and N84° on the northern side (Fig. 17). The orientation of the frontal part of the iconostasis and altar area is N001°, and the northern and southern wings of the main church have the

Fig. 16. The main church of St. Simeon—a view from the western wing through the central octagon and the pillar to the eastern wing. Letters A, B and C mark the central symmetry axis of the cathedral drawn in the direction of N100°, along the line connecting the western wing to the pillar; A and C mark the centers of arcs closing the octagon on the west and on the east; B—the pillar; D—the centre of the main apse arch in the eastern wing is displaced by 3° to the east and oriented to N97°.

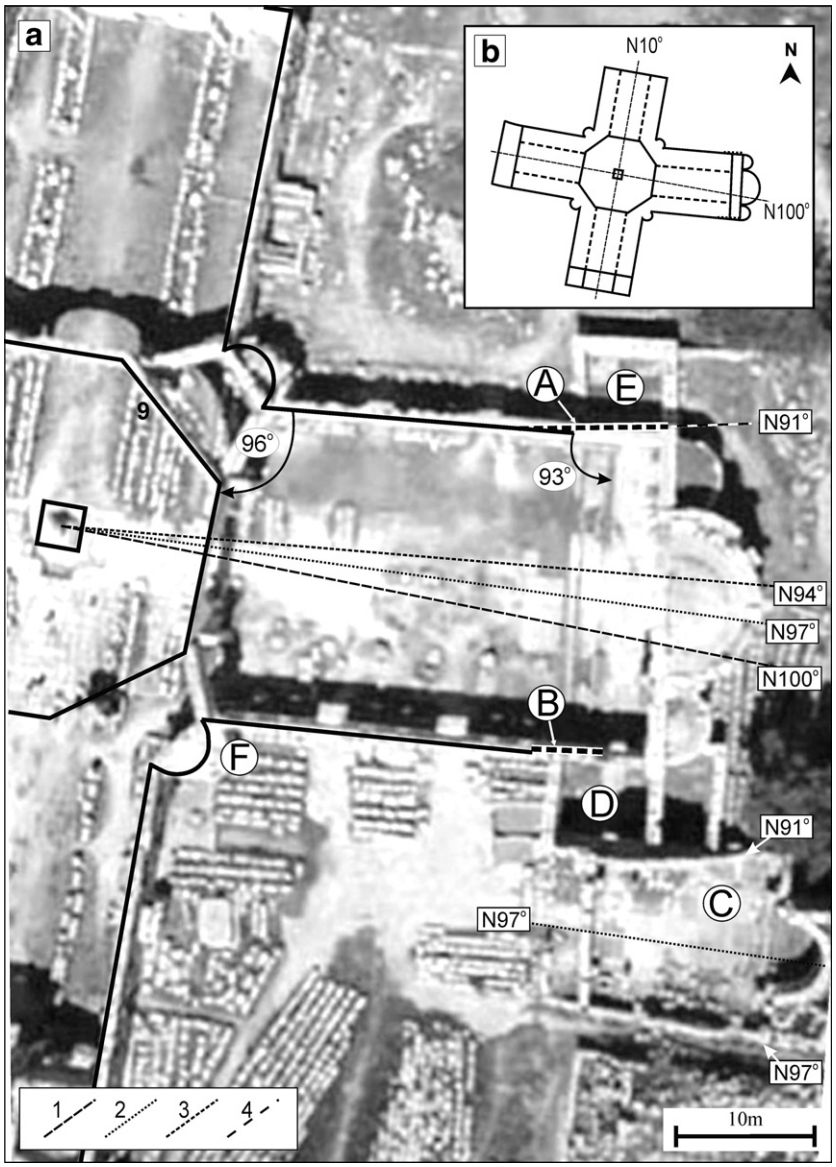

Fig. 17. a—the eastern wing of the main church. 1—axis of symmetry directed from the western wing to the pillar to the eastern wing (Az 100°); 2—axis of symmetry of the eastern wing directed from the pillar to the central part of the eastern wing (Az 97°); 3—axis of 94° representing the orientation of the standing walls in the eastern wing and the position of the stone plates and the mosaic; 4—axis representing the orientation of the old walls (Az 91°); A, B—old wall fragments; C—the main church chapel; E—the *Prothesis*; D—the *Diaconion*. b—general layout of the main church with the N–S and W–E symmetry axes.

azimuth of N10° (Fig. 17). Such geometry of disposition of the iconostasis, altar, main apse, *Prothesis* and *Diaconicon* attests that this part of the church has experienced a counter-clockwise rotation of 9°.

The details of joining between the eastern wing walls and the main apse are of particular importance. The interior of the *Prothesis* contains a survived fragment of an old wall socle constructed of large limestone blocks (*A* in Figs. 17, 18a). The remains of the old wall stretch for 10 m with a strike of N91° and are oblique with respect to the preserved church wall oriented N94°. Near the altar, the old wall is 1 m far from the church wall existing today, but converges and joins it farther to the west. At the site of junction (D in Fig. 18a and b) and west of it, the masonry along the entire height of the standing church wall is older, while its foundation was hollowed in the bedrock (C in Fig. 18a and b). To the east of the junction, the present-day wall was reconstructed in the 20th century, but on the older foundation (B and E in Fig. 18a and b).

A similar pattern is observed inside the opposite, southern wall of the eastern wing: there is a fragment of old wall base, the same as the one found in the *Prothesis* (B in Figs. 17, 18c). The old wall, having a present-day height of two stone blocks and an azimuth of N91°, is oblique with respect to the recent wall that has an azimuth of N94° and stands 0.3 m apart. In the west, the old wall base joins the foundation of the recent wall hollowed in the bedrock. The old wall fragments in the near-altar area bear evidence of a counter-clockwise deformation of the eastern wing by 9° (Fig. 17). An important fact to consider is that the old wall fragments are perpendicular to the iconostasis, altar, and the apse, while the present-day walls join them at an angle

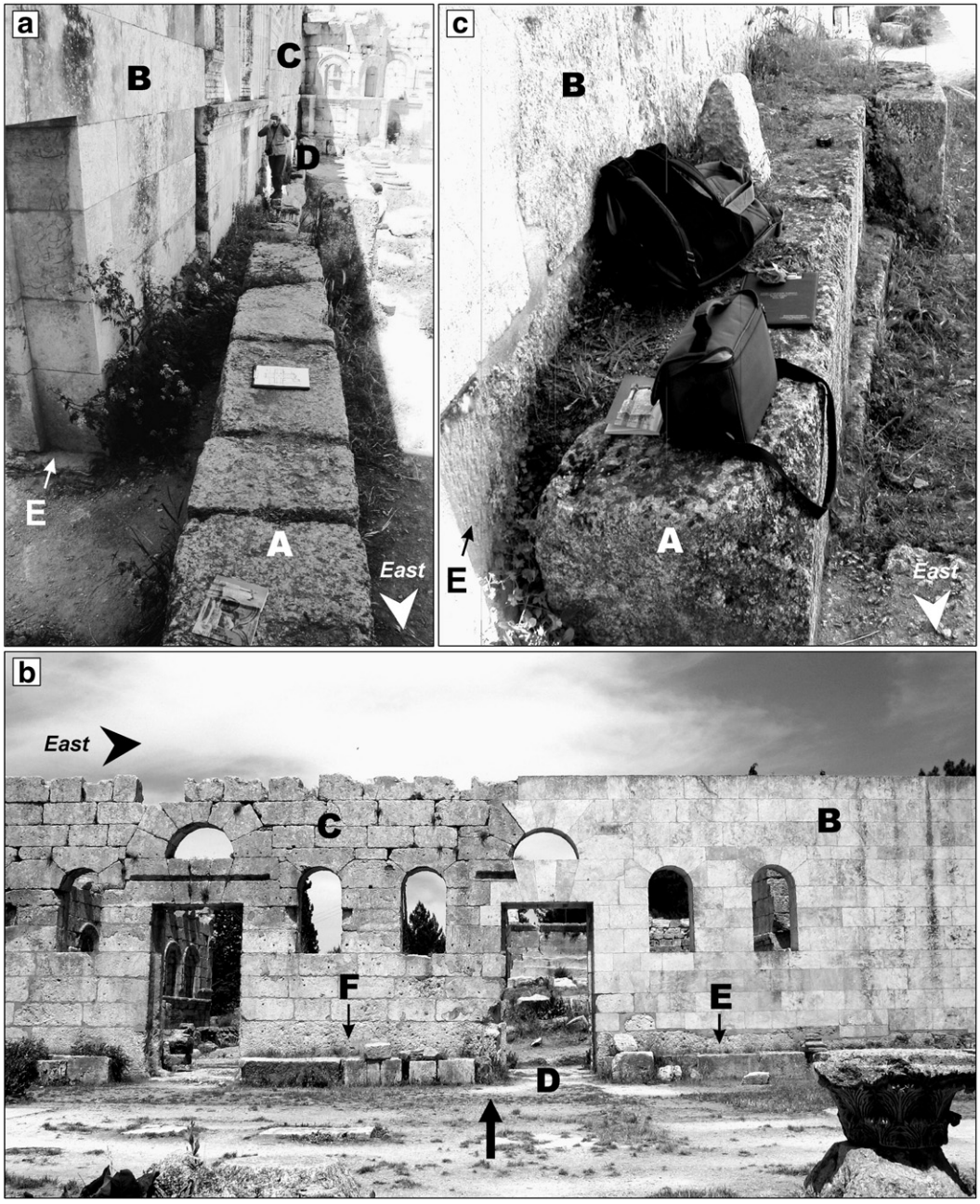

Fig. 18. Old wall fragments in the eastern wing of the main church a—the northern wall of the eastern wing, a view from the Prothesis. (A—the old wall, B—the wall with the masonry restored in the 20th century, C—the wall existing today with the old masonry, D—a part of the old wall fragment joining the wall existing today, E—old foundation, based on which the walls were reconstructed in the 20th century). b—the northern wall of the eastern wing: a view from inside (C—the wall existing today with the old masonry, D—a part of the old wall fragment joining the wall existing today, E—old foundation, based on which the walls were reconstructed in the 20th century, F—a part of the monolithic foundation hollowed in the bedrock) c—the southern wall of the eastern wind, a view from inside (A—the old wall, B—wall with the masonry restored in the 20th century, C—the wall existing today with the old masonry, E—based on which the walls were reconstructed in the 20th century).

of 92–93°. This implies that the iconostasis, the altar, and the main apse, with the adjoining *Prothesis* and *Diaconicon*, composed a unique ensemble with the old wall fragments and were all built concurrently. Therefore, the counter-clockwise rotation of the altar and the main apse by 9° was accompanied by the curving and destruction of the old walls, preserved today as fragments only.

Within the area of joining the iconostasis, segments of the present-day walls (B in Fig. 18*a, b* and *c*) were rebuilt in the 20th century on the older wall foundations (E in Fig. 18*a, b* and *c*). Hence, we can distinguish two generations of differently oriented walls within the altar area in the eastern wing: fragments have remained only from walls of Generation 1, oriented N91°, while walls of Generation 2, existing today, have the azimuth of 94°. Both generations are old and were destroyed in the past. The walls with the azimuth of 91° (Generation 1) are perpendicular to the altar and together with it, apparently, once were parts of the single design. In Generation 2, the walls have

the azimuth of 94° and join the altar obliquely, at an angle of 92–93°, thus implying a later time of construction than in Generation 1.

Apparently, the effects of curving and destruction of the older walls of Generation 1 were eliminated during some early restoration activity in the church, when lateral walls were rectified, but the central apse and the altar remained asymmetrically turned counter-clockwise. The walls of Generation 2 were erected in the course of that ancient restoration, but their near-altar portions were in the later ancient period destroyed again and have taken their today's appearance in the 20th century only.

The main church chapel (C in Figs. 11; 17) also provides examples of bends resulting from seismic deformation. The northern wall of the chapel is 19 m long and strikes N91°, while the southern wall is 1 m shorter and oriented N97°. The central axis of the chapel is parallel to the southern wall and has an azimuth of N97°. Therefore, the northern wall of the chapel turned counter-clockwise by the same angle of 6°. The northern wall, like the adjoining walls of the *Diaconion*, bears indications of very strong seismic impacts and was curved arch-wise to the north (counter-clockwise) in the same manner as the eastern wing of the main church (Fig. 17). The turning of the northern wall of the chapel by 6° to the north (in the counter-clockwise direction) produced dislocation of the chapel altar by 1.4 m. The southern wall of the chapel is not deformed, but bears evidence of ancient restoration and is parallel to the walls of the Convent built in a later period.

The chapel of the Baptistery has the same features as the main church chapel: the northern and southern walls of the chapel are not parallel one to the other, but diverge by 1.5 m near the altar area.

Summing up this evidence, we arrive at the following:

- The western wing of the main church

1. Flank terminations of the loggia walls have clear traces of seismic destruction and are curved arc-wise by 9° to the north in the clockwise direction. The greatest amplitude of the curve is ~3 m in the northern direction. A considerable curve is recorded in the wall of the structure located 50 m west of the loggia down-slope.

- The eastern wing of the main church

1. The symmetry axis of the eastern wing is N97° and rotated 3° to the north (counter-clockwise) with respect to the same axis of the entire church (N100°).
2. The eastern walls existing today and column bases (N94°) rotated by 6° counter-clockwise with respect to the axis of the western wing of the main church and the octagon (N100°). The greatest displacement in this case is ~3 m to the north. Today, the walls preserved in the eastern wing are oblique to the frontal part of the altar (at an angle of 92°). The stone slabs on the floor of the eastern wing and the octagon, like the later age mosaics were paved during the 10th century restoration activity and have the same orientation of N94°.
3. The fragments of old walls remaining at the junction with the near-altar area (N91°) are bent counter-clockwise by 9° with respect to the axis of the western wing of the main church and the octagon (N100°). The greatest displacement is ~4 m in the northern sector. The main apse, iconostasis and altar, with the *Prothesis* and *Diaconicon* adjoining to them, are perpendicular to the old walls, indicating the contemporaneity of their construction. The main apse and the altar, together with the neighboring structures, are turned 9° counter-clockwise. The greatest displacement of the old wall bending in the altar part is ~4 m to the north.
4. Walls of two generations were identified in the near-altar area of the eastern wing. One generation is older and only fragments preserved of it are oriented N91°. The other generation is younger and its walls are standing now (azimuth of N94°), despite bearing traces of destruction of their near-altar part. Portions of these were restored in the 20th century.

- The chapel of the main church

The northern wall of the main church chapel (N91°) bears clear traces of seismic impacts and is arch-wise bent to the north (in the counter-clockwise direction) by 6° with respect to the central axis of the chapel that is oriented N97°. The southern wall of the chapel is oriented N97° and parallel to its central axis and to the walls of the Convent. The displacement is ~1.4 m. The northern wall of the chapel (the azimuth of N91°) is parallel to the fragments of old walls revealed in the near-altar part of the eastern wing of the main church, while the southern wall of the chapel (azimuth of N97°) is parallel to the pattern of plates and mosaics on the main church floor paved in the 10th century.

5. Seismic history of the St. Simeon Monastery (Qal'at Sim'an)

Very brief descriptions of seismic deformations in the St. Simeon Monastery are provided in Sbeinati et al. (2005) and Meghraoui et al. (2003). According to these authors, the monastery was destroyed by the earthquakes of 526 AD, 1137 (M=7.4), 1170 (M=7.7), 1719 and 1822 (M=7.4). Apparently, the monastery was severely damaged also by the earthquake of 854 AD (M=7.5). Unfortunately, no chronicle source gives any direct indication of the specific earthquake that caused the destruction of the St. Simeon Monastery. Therefore, the indirect evidence must be analyzed to identify the historical earthquakes responsible for the destruction of the monastery.

By the early 5th century, the octagonal memorial structure with a dome was erected around the central pillar from which St. Simeon preached. However, the description given by Evagrius after his visit to the monastery in 560 AD mentions an open atrium-yard in the place of the roofed memorial. Based on this, Tchalenko (1953) suggests that the monastery could have been destroyed by the events of 528 and 551, and, probably also by some other unreported earthquake between 490 and 560. Moreover, Tchalenko (1953) mentions that the reconstruction of the monastery late in the 6th century could have a relation to restoration after earthquake damages. Supposedly, some damage of the monastery could have taken place late in the 10th century (Tchalenko, 1953). The majority of the data attest that the dome and possibly the octagonal memorial pavillion over the pillar were destroyed between 490 and 560, but the monastery was totally

ruined between 560 and 976 (Krenker, 1939; Tchalenko, 1953). The earthquakes of 1114, 1157 and 1170 could be responsible for the destruction of the arc in the southern part of the octagon (Tchalenko, 1953).

The studies of the last decade have provided new and abundant evidence concerning historical seismicity in the Eastern Mediterranean, including the area of junction between the Levant and East-Anatolian Fault Zones (Ben-Benahem, 1991; Ambraseys and Melville, 1995; Ambraseys and White, 1997; Meghraoui et al., 2003; Ambraseys, 2004, 2005; Sbeinati et al., 2005). From this new information, we can identify about ten seismic events that could have a destructive impact on the structures of the St. Simeon Monastery and fortress.

However, we believe that plastic deformations of the wings in the main monastery church and in both chapels must be probably related to the impact of permanent co-seismic or post-seismic movements along the St. Simeon Fault, and not to the ground shaking generated by strong yet distant earthquakes. Therefore, to define the seismic event that caused the deformation of walls in the main church and other monastery buildings, it is crucial to identify the earthquakes that possibly reactivated the St. Simeon Fault.

In order to identify such events, we assume that the earthquakes generated by the St. Simeon Fault can be recognized among the entire bulk of historical evidence as those having much greater intensity in Aleppo than in Antioch or Seleucia. Our assumption is based on the following aspects.

The St. Simeon Monastery is located 72 km and 90 km to the west–southwest of Antioch and Seleucia, respectively, (Fig. 1). The LFZ, consisting of 4 to 5 large segments at least, each capable of generating strong earthquakes, runs between the St. Simeon Monastery and Antioch (Fig. 1). Moreover, the cities of Antioch and Seleucia themselves are located on the main branch of the EAFZ that also generated strong earthquakes (Fig. 1). We can base on this to suggest that most likely these faults, and not the St. Simeon Fault, were responsible for the earthquakes that destroyed Antioch and Seleucia. As such, these faults are not the main concern for the purpose of our study. Besides, we believe that supposed location of the sources of some historical earthquakes on the St. Simeon Fault can be ruled out at once, as their intensities in Antioch appear higher than for Aleppo.

The city of Aleppo is located 30 km to the east–southeast of the St. Simeon Monastery (Fig. 1) and the St. Simeon Fault is the nearest large active fault. Strong seismic deformations in the monastery caused by an earthquake on the Ghab segment are rather improbable, as the segment is 60 to 70 km far from the monastery. To identify a historical earthquake with its source on the St. Simeon Fault, evidence of destruction in Aleppo is therefore much more important (particularly if the damage is reportedly very strong in Aleppo, but weak or not recorded in other cities).

Based on the above considerations, the destruction of the monastery can be related to the following earthquakes, likely associated with the St. Simeon Fault.

- The earthquake of November 29 in 528/529 with $M=7.5$ (Intensity XI) that killed 140,000 people; the city and the fortress of Aleppo were totally destroyed. At the least, this event could destroy the dome and the octagonal memorial pavilion over the pillar and cause other serious damage in the monastery.
- The earthquake of 587/588 with a magnitude of $M=7.0$ that killed 60,000. The Aleppo Fortress was destroyed completely, but in Antioch the intensity of this event was only VI to VII.
- The earthquake of 881 with a magnitude of $M=6.5$ that caused strong damage in Aleppo.

The two last events, together with the plausible impact from the earthquake of 854, could have destroyed the monastery to an extent that necessitated its reconstruction in 976–986.

- The earthquake of January 21, 1626 with intensities VIII–IX in Aleppo, VIII–IX in Gaziantep, VI–VII in Hama and VI in Damascus that occurred either on the St. Simeon Fault, or on the EAFZ.
- The earthquake of 1822 with a magnitude of $M=7.2$, which, by the data of Ambraseys and Melville (1995), was accompanied by surface rupturing. The epicenter could be localized on the northern segment of the St. Simeon Fault (Ambraseys and Melville, 1995) or, according to Sbeinati et al. (2005), on the Ghab segment. This event might have additionally deformed the monastery.

6. Discussion

With very few exceptions, Christian church altars were oriented approximately to the east. The orientation to the east was determined by the first ray of sunlight on the day of the Saint to whom the church was consecrated (Benson, 1956; Rappoport, 1994). In the meantime, deflections from the eastern direction by 10° and even greater angles were quite possible. An example is the Church of San Procolo di Naturno (7th c. AD, Rome), where, as a result of builders' error, the altar orientation was deflected by 16° to the north. To rectify this, the altar was turned by 6° late in the Middle Ages (Codebò, 1996, 2000). Therefore, the position of altar in the St. Simeon Church deviated by ~10° from the east can be regarded as an ordinary phenomenon. The extraordinary feature is the deflection of the eastern wing from the cruciform plan, as well as other bends and structural discordances. Different explanations and various models have been suggested to interpret the visible deflection of the eastern wing. Traditionally, local population has considered this deflection as a Christian symbolic, believing that the church was designed with a bend to the left side, as the Savior bowed His head to the left on the cross. This explanation will not be commented here.

There is also an opinion about a miscalculation made during the construction, because it was started from diverse ends of the church concurrently. Agreeing with this explanation in general, others consider that the eastern wing was adjoined to the pillar and the octagon first. After it was completed, the builders had to turn the design of the western, and, correspondingly, the northern and the southern wings considering the proximity of a

steep slope and, as a consequence, limited space available for construction in the west. Indeed, the space in the west of the church is limited by the steep slope and the western wing rests on the arcade built on this slope. However, we think that such bending of an entire church with respect to its eastern wing could not help to resolve this problem and would even additionally reduce the space available in the west. With the high rate of performance of the Early Byzantine architecture and engineering, and keeping in mind the religious and political importance of a church of that grandiose size, we consider these versions of *construction errors* unlikely. Solid arguments for the contemporary start of construction of wings to all four sides are also in conflict with such explanations (Butler, 1920; Krenker, 1939; Tchalenko, 1953).

In our view, Butler (1920), Krenker (1939) and Tchalenko (1953) proposed the most forcible explanation suggesting that the construction of all four wings was started in the same time with the building of the central memorial octagon, and the latter, together with the pillar of St. Simeon, served for coordination of the four wings in space. We will refer to this version as to the *architectural* one.

According to the *architectural* version, the accuracy of placement of the pillar into the octagon center, reciprocal perpendicularity of walls of the three wings and the religious importance of this huge church exclude the possibility of a construction error. Therefore, the deflection is deemed to be *an element of architectural design*. The orientations of walls and arcs in the octagon supposedly were determined by the position of the rectangular base under the St. Simeon's pillar, the sides of which strike with the azimuths of N18° and N108°. Later, basilicas of the four wings were added to the octagon. The northern, southern and western wings did not have any ritual importance and as such were oriented by the octagon edges, i.e., eventually, by the directions of the rectangular pillar base. As a consequence, the eastern wing would appear deflected by 10° from the east, hence, as this part had to be used for service, it was intentionally turned 3° nearer to the east. The only divergence of opinions is that some of the researchers think this was the initial design, while others believe that the idea of turning the eastern wing arose in the course of construction, or a reconstruction.

However, we think that the *architectural* versions encounter problems failing to explain all structural deformations in the monastery, and particularly the turn of the altar in the counter-clockwise direction and the orientation of the old wall fragments.

The problems of the *architectural* versions forced us to search for a *seismic* explanation of the described distortions in the church and other structures of the St. Simeon Monastery. We based our seismic scenarios on the measurements of monastery structure deformations, as described above, correlated with the analysis of high tectonic activity of both sub-segments of the St. Simeon Fault and strong seismic effects the buildings of the St. Simeon Monastery and Telanissos experienced in the past.

In the following, three major questions will be discussed:

- What facts could attest in favor of seismic deformation of the monastery structures, and how reliable are these facts?
- When could the seismic deformation of the monastery structures have happened?
- What was the mechanism of seismic deformation of the monastery structures and how did it originate?

The *seismic* scenario is based on the assumption that walls in different parts of the monastery, including the eastern wing, could change their positions in space under the impact of deformations caused by strong earthquakes or by post-seismic creep so that their present-day positions do not correspond to the initial ones. This assumption is supported by the facts we yielded from old wall findings, rotation of the main apse and the altar and differential spatial orientation of individual structures. To consider plausible scenarios of monastery structure deformations, we need to base on some idea about the orientations the main wings of the church could have at the moment of construction, i.e., before the seismic impacts. Two models can be considered in this regard.

6.1. Model 1 (minimum seismic effect)

This model (Fig. 19) incorporates an assumption made in the *architectural* version about the intentional deflection of the eastern wing by the builders as mentioned by Butler (1920), Krenker (1939) and Tchalenko (1953). As commonly considered by the *architectural* approach, the planned deflection was by 3° and the axis of the eastern wing was oriented N97°. We decided to follow an even more conservative approach in favor of the architectural model and assume that the walls existing today and oriented N94° were the ultimate realization of the old design conception. In such case, the seismic impact in the eastern wing could be limited to the bending of old walls, main apse and the altar only by 3° to the north (the difference between the orientation of now standing (N94°) and old (N91°) walls) that had an amplitude of 1 m. The western wing deflected by 9° to the north with an offset of 3 m. The deflections of walls in the chapels of the main church and the Baptistery corresponded to 1.4 m and 1.5 m, respectively. We do not think it is possible to suggest that the eastern wing was orientated N91°, i.e., set even more easterly in the initial design, as this would imply that designers of the 10th century reconstruction positioned new walls at N94°, obliquely to the earlier walls (N91°) and, moreover, deflected the constructed structures to a direction opposite to the east.

6.2. Model 2 (maximum seismic effect)

This model (Fig. 20) provides for originally symmetric design of all four wings of the main church, where the eastern wing, like the western one, was oriented N100°. In such case, the maximum angle of later deflection of the eastern wing to the north was 9° and the greatest offset it produced was ~4 m. In this scenario, western wing deflections would again correspond to an angle of 9° and horizontal offset by 3 m, while deformations in both chapels would be the same as in Model 1.

According to Model 1, the most credible indicators of seismic deformation were found in the altar section of the eastern wing in

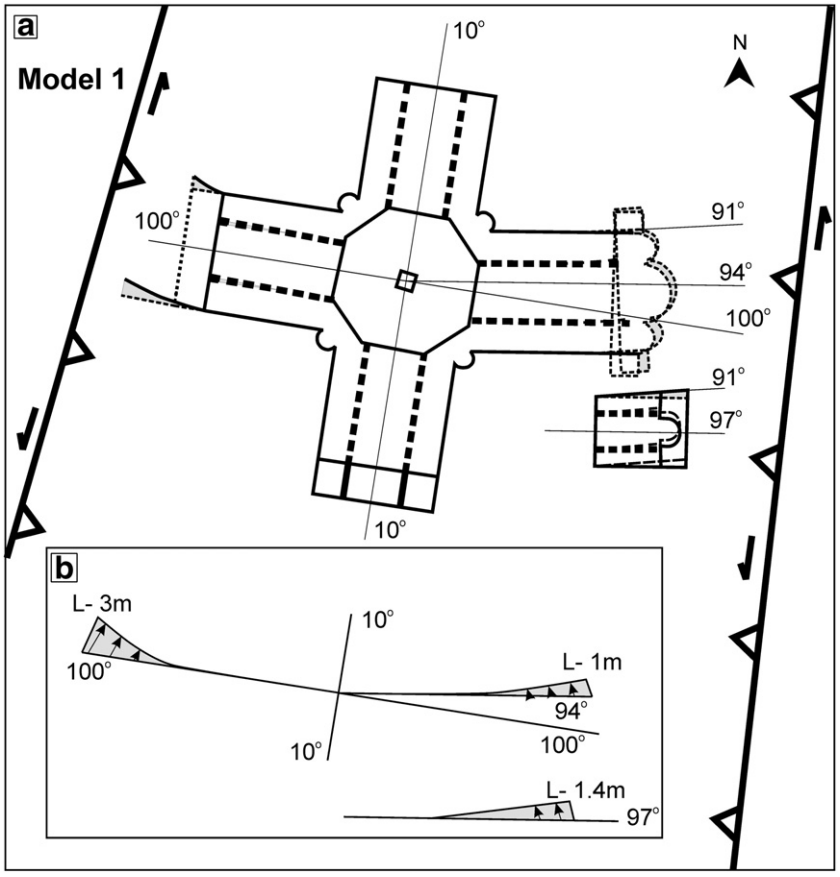

Fig. 19. Model 1, illustrating a seismic version explaining deformations in the main church and the chapel. a—the model; b—the supposed strain diagram of the main church and the chapel. The position after the seismic impact is hatched.

the main church and at loggia wall terminations in the western wing. The old wall fragments provide a reliable evidence of bending deformation experienced by the entire altar section of the eastern wing in the counter-clockwise direction. On one end, the old walls are perpendicular to the iconostasis, while on the other they adjoin the existing walls in the point where the latter were hollowed in the bedrock (Figs. 17 and 18). There are clear signs that the counter-clockwise rotation incorporated the entire altar section and the old wall fragments concurrently, which is an important fact. The northern wall of the main church chapel is parallel to the old wall fragments in the eastern wing altar area and was also bent by 1.4 m to the north. The identified deformations cover a zone up to 50 m wide from the north to the south and 25–30 m wide from the west to the east, and the offsets they produced increase eastward to up to 1–1.5 m.

The indications of deformational bends are likewise apparent at the end of the arcade, supporting the loggia in the western wing of the church, where the remains of walls are bent by 9° clockwise, which, given that the deformed zone is up to 16 m wide, yields an offset of 3 m. Deformation traces can be noticed even farther to the west, in the walls of the rectangular structure on the slope under the loggia.

We can suggest the following scenario of deformations. A strong earthquake or a post-seismic creep deformed the near-altar part in the eastern wing. The bedrock-hollowed base of the main apse turned counter-clockwise by 3°, together with all altar structures. About 10 m-long wall sections adjacent to the altar were also turned by 3° and were set into a new orientation of N91°. Apparently, the earthquake ruined the curved wall sections at the kink points, but in the course of later restoration works the walls were rectified to their present-day appearance and the azimuth of N94°. The walls of the main church chapel were damaged severely. The northern wall adjoining the *Diaconicon*, remained standing, but was bent to the north together with it, while the southern wall was destroyed. The southern wall was later restored, but in a direction parallel to the walls on the Convent building. The flank of the western wing of the main cathedral was strongly damaged and apparently this necessitated the moving of the entrance to the southern wing.

Model 1 has been based on these facts; according to it, the established deformations of horizontal curving were concentrated within narrow bands, covering only the near-altar part of the eastern wing of the church and an area adjacent to the western wing. The horizontal offsets of the revealed seismic distortions of bending correspond to 1–1.4 m and 3 m on the eastern and western flanks of the main cathedral, respectively. Within the bands, deformations become more intense closer to the sub-segments of the St. Simeon Fault that bound the Sim'an Ridge on both sides. A possible interpretation and the resulting stress diagram for Model 1 are shown in Fig. 19.

According to Model 2 (Fig. 20), seismic deformation is assumed as the cause of not only the above curves in the near-

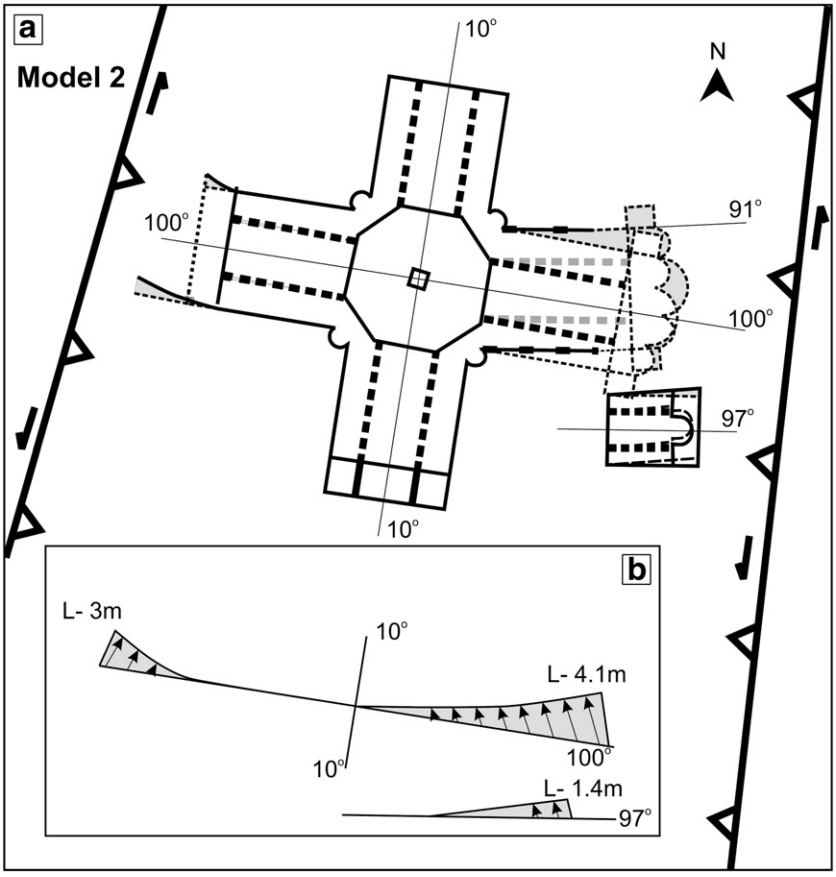

Fig. 20. Model 2 illustrating a seismic version explaining deformations in the main church and the chapel. a—the model; b—the supposed strain diagram of the main church and the chapel. The position after the seismic impact is hatched.

altar area, but also the general bend of the entire eastern wing by 9° with respect to the other parts of the main church. With this assumption, the eastern band of deformations widens up to 50–55 m, while deformation amplitudes show the tendency to increase both eastward and westward. The amplitudes of bends of the eastern and western wings reach ~4 m and 3 m, correspondingly. The integrated width of the deformation zone thus corresponds to 170–200 m. Interpretation and resulting stress diagram for Model 2 are shown in Fig. 20. Model 2 uses all facts included in Model 1, but incorporates many additional, rather hypothetical factors, which make it less credible compared to Model 1.

As shown above, the southern wall of the eastern wing is 3 m longer than the northern one. Model 1 assumes that the builders knowingly curved the eastern wing, so that the northern and southern walls had different lengths originally. As a result of later seismic deformation and rotation of the altar by 3° the southern wall was additionally extended slightly.

Model 2 provides for the equal initial lengths of both walls in the eastern wing. In such case, with the 9° rotation of the altar the southern wall could be extended and the northern shortened so that the difference of their lengths makes 3 m presently. Hence, presence of any traces of extension within the southern wall and/or shortening in the northern wall is an important question to assess the credibility of Model 2.

Unfortunately, repeated earthquakes, wars and subsequent reconstructions have strongly altered the appearance of both walls. Our visual inspection allowed recording just individual traces of the inferred change of wall lengths in the eastern wing.

The plan of the eastern wing (Fig. 21b) drawn before the reconstruction of the monastery in the late 20th century (Butler, 1920) shows that a 3 m-long section of the southern wall (marked B in Fig. 21a) has twice smaller width than any other wall. In the meantime, the opposite section of the northern wall (C in Fig. 21a) is slightly pushed inside the octagon contour. At the site marked A in Fig. 21a, we noticed a break that had extended the bedrock-hollowed foundation of the southern wall by 0.5 m (Fig. 21b). These observations are apparently insufficient to support all assumptions made in Model 2, however, the cleaning of the wall foundation and further investigation might be able to disclose other evidence of extension in the eastern wall.

Model 1 assumes single deforming impact (strong earthquake or post-seismic creep) and one stage of restorations performed in the 10th century. Model 2 assumes the possibility of several episodes of strong seismic effects that led to the deformations and curves of the main church structures, as well as at least two stages of restoration activities, one late in the 6th and one in the 10th century.

It is difficult to determine the age of seismic deformations in the main church and other structures of the St. Simeon

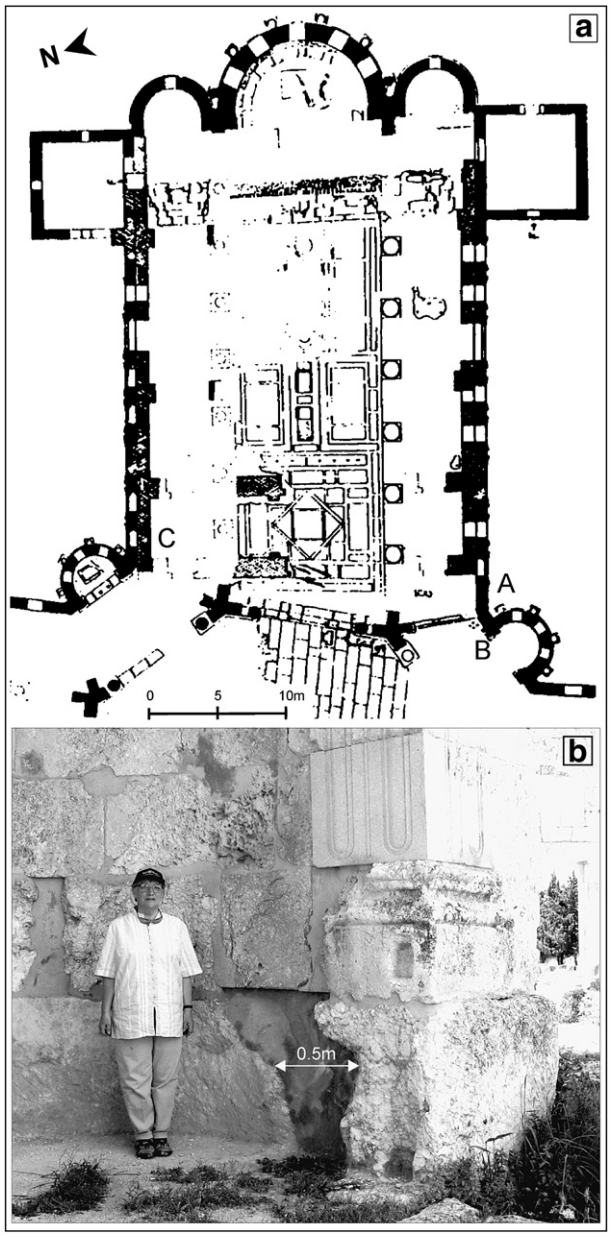

Fig. 21. a—plan of the eastern wing prepared before the reconstruction of the monastery late in the 20th century (Butler, 1920). Point B indicates the location of the photograph shown in Fig. 21b; b—break that produced the extension by 0.5 m in the foundation of the southern wall of the eastern wing.

Monastery as the available historical and archaeological data are scarce and as the monastery has been remaining ruined during the last 800 years and many important details could have been lost during the repeated reconstructions.

We can make just few suggestions to constrain the time of the deformations. Undoubtedly, the damage was caused to the chapels in the main church and the Baptistery, therefore their construction in late 5th or early 6th centuries pre-dates the seismic events.

The stone plates and mosaics on the eastern wing floor were paved in the 10th century and are parallel to the walls of the eastern wing existing nowadays. Hence, the 10th century restoration activities can post-date the age of deformations that caused the altar to curve. Additionally, this post-date is confirmed by the fact that the fortress walls built in the 10th century do not bear any traces of seismically-induced bending deformations despite other kinds of seismic damages are evident.

The resulting interval between the early 6th and late 10th centuries is rather large and can include many strong earthquakes, the effects of which could have caused these deformations. We can try to reduce their number. Tchalenko (1953) mentions that the construction of the chapels and the Baptistery was completed immediately before the strong earthquakes of 526/528 and Evagrius, who visited the monastery in 560, described it in intact condition. Besides, Tchalenko (1953) mentions the restoration activity performed late in the 6th century, which could take place before the Evagrius' visit.

Most probably, the earthquake of 528/529 with a magnitude of 7.5 was one of the causes of the co-seismic or post-seismic deformations in the monastery. This event must be distinguished from the very strong earthquake of 526 (M=7.3) in the southwestern part of the EAFZ that destroyed Antioch and killed many in this city. The effects of the earthquake in 528/529 are reported by many historical chronicles attributing the greatest damage to the city of Aleppo. This implies that the epicenter was likely close to Aleppo and possibly located in the zone of the St. Simeon Fault Zone. Apparently, the central octagon dome collapsed and the walls and the entrance in the western wing were destroyed during the earthquake. The damaged walls could be re-laid during restoration activities, when the lateral walls in the most distorted near-altar part of the eastern wing were straightened so that the bases of the original, deformed walls appeared beside. The entrance into the cathedral was shifted from the destroyed western to the southern wing, but the dome over the central octagon was never restored and the latter turned to an atrium. However, one cannot exclude other strong earthquakes in the interval between the completion of monastery construction in 490 and the visit of Evagrius in 560, the memory of which, as Tchalenko (1953) believes, could be erased by the events of 526 and 528.

Direct impact of one or several seismic events, or the post-seismic creep could additionally deform the monastery also in the period between the visit of Evagrius in 560 and the 10th century restoration. The earthquake of 587/588 could have been one of such events. Later destructions, caused by the Arab invasions and the earthquakes of 746, 757, 854, 881 and 963 turned the greater part of the monastery into ruins. When Byzantium regained its control over the monastery, the eastern wing of the main cathedral, the chapel and some other structures were restored. The new stage of destruction was related to the conquest of Qal'at Sim'an by the Arabs and the consequent series of strong earthquakes in the 12th century, and then in 1114, 1170, 1408 and 1822. These calamities destroyed or damaged even the structures that had been erected or rebuilt in the 10th–11th centuries. Along with this, seismic damages in the main cathedral could be accumulating, which is attested by the destruction of fortress walls built late in the 10th–early in the 11 cc. We can suggest that the earthquakes of 528 (M=7.5), 587 (M=7.0) and 757 (M=7.0), which most probably happened

on the St. Simeon Fault, could be those responsible for the seismic deformations of bending. There is no doubt that the strongest seismic events that repeatedly caused complete destruction of Antioch and the broader across Northern Syria in 500 (M=7.0), 526 (M=7.0), 565 (M=7.0), 678 (M=7.7), 746 (M=7.3) and 854 (M=8.0) all had their contribution in the considerable destruction of the monastery. Besides, it is quite probable that other strong historical seismic events at the St. Simeon Fault still remain unknown to us.

We will try to analyze a possible mechanism of the seismic deformations recorded in Telanissos and the St. Simeon Monastery. Intense rotational deformations can develop at the sites confined between two strike-slip faults (Nelson and Jones, 1987; Dickinson, 1996; Randall et al., 1996; Harris et al., 2002). We observed rotational deformations in our study of destroyed buildings both in Telanissos (Deir Siman) and in the St. Simeon Monastery, and we can distinguish two different kinds of such effects. Numerous turns of individual stone blocks can be related to the first type of distortions that are quite common in Telanissos and in the St. Simeon Monastery (Fig. 12). The second type must be related to bending phenomena and rotation of the entire structures, for instance, the altar or 10 m or longer walls in the St. Simeon Monastery (Figs. 17, 19 and 20).

We recorded 35 cases of rotation in Telanissos and 19 in the St. Simeon Monastery. Measuring and analyzing rotation directions, we recorded the initial positions in space, as well as the geometry and the dimensions of turned blocks, and the horizontality of their positions before and after the turn. Systematically oriented mass rotations of stone blocks can be caused only by ground movements in a strong earthquake (Korjenkov and Mazor, 1999). Similar effects were observed by the studies in the zones of recent strong earthquakes (Arnold et al., 1976; Berberian, 1976; Karakhanyan and Balassanian, 1992; Yegian and Ghahraman, 1992) and inspections of historical structures damaged by the earthquakes of the past (Korjenkov and Mazor, 1999; Croci and Biritognolo, 2000; Korjenkov and Kaiser, 2002; Korjenkov and Mazor, 2003; Bottari, 2003).

Karakhanyan and Balassanian (1992) and Yegian and Ghahraman (1992) provide some estimates of gravestone rotation mechanism during the 1988 event (M_S=6.9) in Armenia. Shaking-table tests enabled them to conclude that under the impact of the twisting moment of the horizontal inertia force, blocks initially facing to the east turned by 20–30° and took a new position perpendicular to the direction of earthquake motion and eventually to the scarp of the generated surface rupture (Karakhanyan and Balassanian, 1992). This suggests a strong azimuthal variation of the ground motions in the *near-field* during the Armenian earthquake in 1988. A similar observation was made by Arnold et al. (1976) for the 1971 San Fernando earthquake and by Berberian (1976) for the 1931 earthquake in Salmas (Iran).

Fig. 22 shows a scheme that represents the results of some measurements of block rotation directions in the St. Simeon Monastery and Telanissos. A few of the turned blocks recorded in Fig. 22 are shown in Fig. 12. Our analysis of block rotation directions indicates that in the St. Simeon Monastery and in Telanissos stone blocks rotated clockwise in the N–S oriented walls and counter-clockwise in the W–E oriented walls. Along with this, the rotated blocks tended to take positions approaching the vector of seismic ground movement, i.e., perpendicular to the active fault zones bordering the Sim'an Ridge (Fig. 21). Where the blocks were initially oriented nearly perpendicular to the fault, we recorded their lateral offsets away from the fault (g in Figs. 12 and 21). Some of the rotated blocks bear clear traces of restoration in the ancient time (like b in Figs. 12 and 21), and some look perfectly intact. Apparently, this attests to repeated strong seismic events that struck the monastery during the historical period.

Therefore, we can suggest that rotations of individual rectangular blocks of structures in Telanissos and St. Simeon indicate proximity of the surface rupture and that in turning the longer axes of rectangular blocks tended to take positions most approaching to the perpendicular to the surface rupture. At the present, it is difficult to say whether the rupture produced a surface break. Most probably, the rupture run along the side of the Sim'an Ridge, which is the supposed location of the main branches of the active faults. However, there has been no way to clear up this question, as intense agricultural activity has been led in this area since ancient time. Palaeoseismological trenching must be performed at the mentioned sites in future.

As mentioned above, bends of not only individual stone blocks, but entire structures of the main apse, altar and lengthy wall fragments are recorded in the area of the St. Simeon Monastery. The band encompassing such turns was up to 100–120 m wide at the least, although by some estimates (Model 2) it could be more than 200 m wide and 300 m long. Apart from such sizable dimensions of the deformation zones, the following facts should be pointed out: i) within an individual zone, structural deformations are of the same kind and bending angles are similar for diverse structures. For instance, both fragments of the old walls and the northern wall of the main church chapel are turned similarly by 9°, although located 35 m apart; ii) the deformations in the eastern wing are similar to those in the western one by the width of distortions band, the angles of rotations and the resulting offsets; iii) northern bends with counter-clockwise rotations are characteristic for the eastern wing deformations, northern bends but with clockwise turns are noticed in the western wing; iv) either on the western, or on the eastern wings, the displacement increases toward the outer sides, i.e., toward the strike-slip faults bordering the Sim'an Ridge.

We can interpret this pattern by plastic deformation of bending or rotation of the block confined between two strike-slip faults. This kind of deformation has been described in many case-studies (Nelson and Jones, 1987; Dickinson, 1996; Randall et al., 1996; Harris et al., 2002), in particular, for the EAFZ that is not far from the St. Simeon Fault (Tatar et al., 2004). Deformation of a block confined between two left-lateral strike-slip faults must give rise to a clockwise rotation (Randall et al., 1996; Tatar et al., 2004). However, the deformation diagrams we obtained for Models 1 and 2 both indicate deformation characteristic of pushing in the SSW direction (Figs. 17, 18). Apparently, this happens because the strike-slip

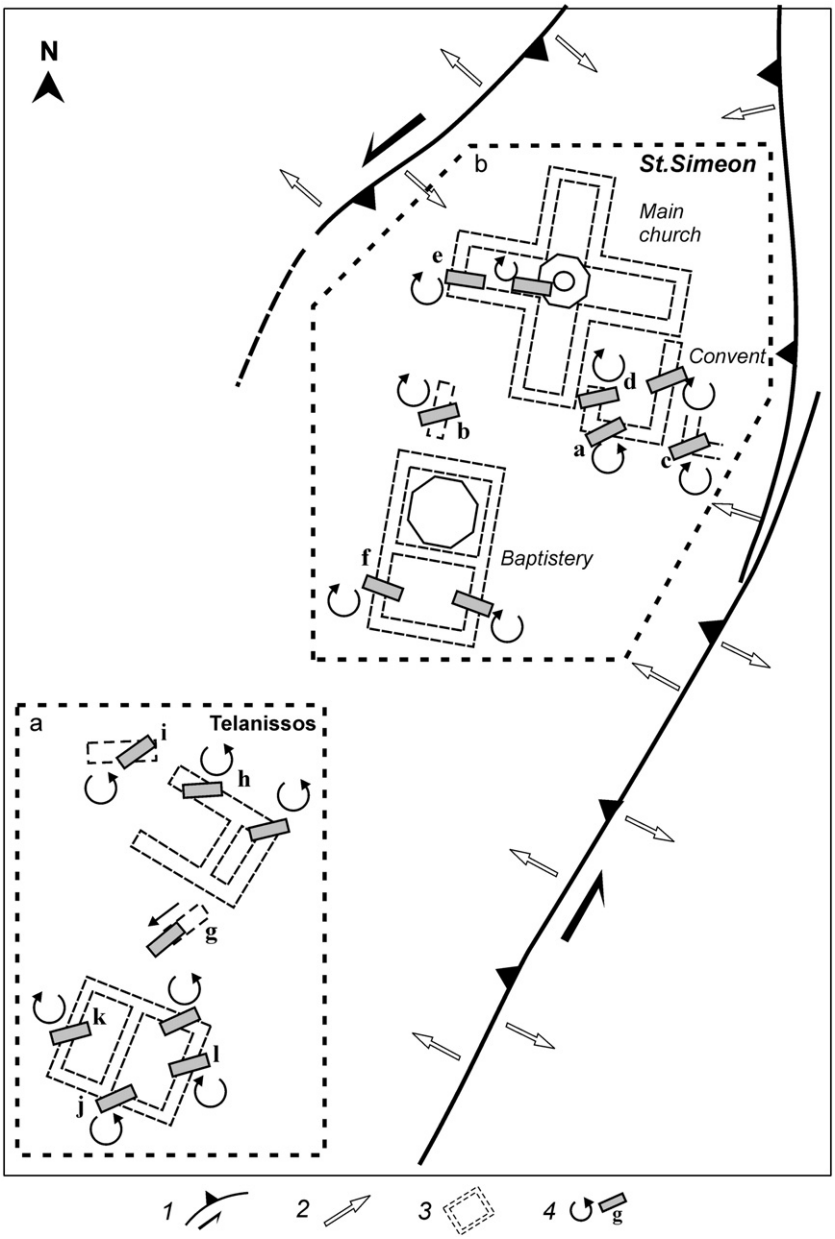

Fig. 22. The scheme representing the results of measurements of stone block rotations (a) in Telanissos and (b) in the St. Simeon Monastery. 1—main active faults; 2—suggested direction of seismic ground movement in an earthquake; 3—some of the large structures, where block rotations are recorded (enlarged compared to the scale of the scheme), the letters denote photos in Fig. 12; 4—block rotation directions.

faults bordering the Sim'an Ridge converge northwards (see Fig. 9a). In such circumstances, the mechanism of *structural scissors* becomes predominant and causes contraction and shortening of the area between the two obliquely oriented strike-slip faults, pushing rocks masses out to the SW (see Fig. 9b). Apparently, this mechanism can produce not only the horizontal overlap of the Sim'an Ridge towards the southwest, but also the transpressive pushing of the entire ridge upward, which forms secondary ruptures resembling a *flower* structure. The localized uplift can also result from an increase of the transverse shortening component determined by the 20–40° deviation of the Sim'an Ridge and its bounding faults from the mean strike of the St. Simeon Fault.

7. Concluding remarks

The situation we observed on the Sim'an Ridge and the bending deformations of structures in the St. Simeon Monastery are not a realization of some initial architectural design, but rather a result of deformation of the entire block confined between the two obliquely joining and active strike-slip faults. If we assume that the curvature of walls in the quadrangular structure down-slope from the western wing of the main church has the same age as the deformations in the church, a reflection of the z-form deformation of the Sim'an Ridge can be recognized in the shape of the wall curvature. The supposed z-shaped deformation could originate from the rotation of the

whole block of the Sim'an Ridge as it was pushed to the south–southwest along the active strike-slip faults flanking the ridge. The bending deformations could originate during strong earthquakes, or, possibly, post-seismic creep. There is no way to establish this presently. This is the seismic scenario, which, in our view, could help to explain the structural deformations in the St. Simeon Cathedral.

The comparison of the *architectural* and *seismic* versions shows that arguments *pro* and *contra* are available for both. The strongest argument in favor of the *architectural* version and against Seismic Model 2 is the absence of any indications of displacement and deformation at the junction of the eastern wing walls with the walls and arcs of the central octagon. Accepting Model 2 (*Maximum Seismic Effect*), we have to assume that the deformation could be plastic and therefore dissipated through the entire length of the eastern wing of the cathedral instead of forming noticeable ruptures and cracks of sliding and detachment. This is possible yet very unlikely. Otherwise, it can be also admitted that any trace of structural deformation at the junction of the eastern wing walls with the walls and arcs of the central octagon were masked by later restorations, which seems to be much more plausible. In any case, seismic Model 2 requires much more assumptions than Model 1.

In our view, the evidence against the *architectural* versions is much heavier than the evidence in support. The architectural scenarios suggest initial designing of a *distorted* cathedral, or forced distortion of its regular shape in the course of construction. The turn of the eastern wing made it just 3° closer to the eastern orientation. We have found facts convincing that the architecture of the considered epoch was tolerant towards departures from the due east orientation and the Byzantine canons did not require to turn a part of the structure to eliminate faults of this kind. In the Church of San Procolo di Naturno such reconstruction was nevertheless realized, but this happened in the medieval Europe, long time after any activity in the St. Simeon Monastery had ceased. Another illustration of the tolerable attitude of the Byzantines with respect to much greater deflections of churches from the orientation to the east is the Aiya Sofia Cathedral in Constantinople. The apse and the altar of this metropolitan church are turned by 40° to the south, while this did not either embarrass the Byzantines, or compel reconstruction of the building from them.

Accordingly, we believe that the *designed* turn of the eastern wing in the St. Simeon Cathedral suggested by the architectural versions is unconvincing both in terms of the formulation of its purpose and the efficiency of the actual turn by 3° achieved in the result.

Eventually, the *architectural* version fails to explain: firstly, the northern bends of the loggia wall fragments in the western wing of the main church, while they are similar to the bends in the eastern wing by offset orientations and amplitudes; secondly, the northward deflections of the old wall fragments in the eastern wing; thirdly, the counter-clockwise turn of the main apse, iconostasis and altar in the eastern wing; fourthly, the distortions of the northern wall in the main church chapel similar to the bending of old wall fragments in the eastern wing.

We believe that the seismic model better explains most deformational features in the main church and other buildings of the St. Simeon Monastery. The structural deformations in the main church focus our attention on studying earthquake-induced plastic deformation in active fault wings and inside intra-fault blocks and on using the derived data for *near-field* seismic impact assessments.

Undoubtedly, the *architectural* and the *seismic* models are both uncertain; either lacks new evidence and requires additional careful study. Clearly, the St. Simeon Fault, St. Simeon Monastery, Qal'at Sim'an Fortress, Telanissos and other *abandoned cities* of the northern karst plateau of Syria are exceptional phenomena, calling for careful preservation and continued study in relation to active tectonics, archaeoseismicity, historical seismicity, palaeoseismicity and local seismic culture. The outcome of such research could give valuable information for active tectonics and supplement databases on rupturing and near-field ground motions of strong earthquakes, engineering seismology, seismic hazard assessment and design of earthquake-resistant structures.

Acknowledgements

The authors are grateful to the staff of GEORISK Scientific Research CJS (Armenia): Y. Abgaryan for her help in editing the manuscript, A. Mkrtchyan, S. Arakelyan, and V. Davtyan for creating GIS databases and 3D models. We thank Dr. Bruno Helly and Dr. Christine Chataigner from Maison de I'Orient Mediterranien (Lyon) for their help in the search for recent publications and consultations on the archaeological studies performed in the area of the St. Simeon Monastery.

References

Altunel, E., Stewart, I.S., Barka, A., Piccardi, L., 2003. Earthquake faulting at ancient Cnidus, SW Turkey. Turk. J. Eart. Sci. 12, 137–151.

Altunel, E., Meghraoui, M., Serdar Akyüz, H., Yalçıner, Ç., Karabacak, V., Bertrand, S., Munschy, M., Ferry, M., 2005. Faulted archaeological man-made structures by the Dead Sea Fault zone in southern Turkey. SRef-ID: 1607-7962/gra/EGU05-A-02362. Geophys. Res. Abstr. 7, 02362 (2005 © European Geosciences Union).

Ambraseys, N.N., 2004. The 12th century seismic paroxysm in the Middle East: a historical perspective. Ann. Geophys. 47 (2/3), 733–758.

Ambraseys, N.N., 2005. The seismic activity in Syria and Palestine during the middle of the 8th century; an amalgamation of historical earthquakes. J. Seismol. 9, 115–125.

Ambraseys, N.N., Melville, C.P., 1995. Historical evidence of faulting in Eastern Anatolia and Northern Syria. Ann. Geophys. XXXVIII (3–4), 337–343.

Ambraseys, N.N., White, D., 1997. The seismicity of the Eastern Mediterranean Region 550-1 BC: a re-appraisal. J. Earthqu. Eng. 1 (4), 603–632 (Imperial College Press).

Arnold, P., Vanmarcke, E.H., Gazetas, G., 1976. Frequency content of ground motions during the 1971 San Fernando earthquake. Research Report R76-3, Mass. Inst. Of Tech. Cambridge, Massachusetts.

Ben-Benahem, A., 1991. Four thousand years of seismicity along the Dead Sea Rift. J. Geophys. Res. 96 (B12), 20,195–20,216.

Benson, H., 1956. Church orientation and patronal festivals. Antiq. J. 36, 210.

Berberian, M., 1976. Contribution to the Seismotectonics of Iran. Part II. Geological Survey of Iran, Tehran. (Report 39, 516 pp.).

Bottari, C., 2003. Ancient constructions as markers of tectonic deformation and of strong seismic motions. 11th FIG Symposium on Deformation Measurements, Proceedings. Santorini, Greece.

Brew, G., Lupa, J., Barazangi, M., Sawaf, T., Al-Imam, A., Zaza, T., 2001. Structure and tectonic development of the Ghab basin and the Dead Sea fault system, Syria. J. Geol. Soc. (Lond.) 158, 665–674.

Butler, H.G., 1920. Ancient Architecture in Syria. Archaeological Expedition to Syria in 1904 1905. Publ. of Prinston University, Leyden.

Codebò, M., 1996. Uso della bussola in archeoastronomia. Atti del XVI Congresso Nazionale C.N.R. di Storia della Fisica e dell'Astronomia, pp. 323–335.

Codebò, M., 2000. Archeoastronomia in Val Venosta: S. Procolo di Naturno (BZ). http://www.archaeoastronomy.it.

Croci, G., Biritognolo, M., 2000. The structural behaviour of the pyramid of Chephren. Proceedings of the International Millennium Congress Archi 2000, Bethlehem, Palestine (http://www.unesco.org/archi2000/papers.htm).

Dickinson, W.R., 1996. Kinematics of Trans-rotational Tectonism in the California Transverse Ranges and its Contribution to Cumulative Slip along the San Andreas Transform Fault System. Special Paper, vol. 305.1. Geological Society of America, Boulder, Colorado.

Ecochard, M., 1936. Le sanctuaire de Qal'at Sem'an: notes archeologiques. Bulletin d'Etudes Orientales, pp. 61–90 (VI).

Ellenblum, R., Marco, S., Agnon, A., Rockwell, T., Boas, A., 1998. Crusader castle torn apart by earthquake at dawn, 20 May 1202. Geology 303–3064 (April).

Galli, P., Galadini, F., 2001. Surface faulting of archaeological relics: a review of case histories from the Dead Sea to the Alps. Tectonophysics 291–312.

Garfunkel, Z., Ben-Abraham, Z., 2001. Basins along the Dead Sea Transform. In: Ziegler, P.A., Cavazza, W., Robertson, A.H.F., Crasquin-Soleau, S. (Eds.), Peri-Tethys Memoir 6: Peri-Tethyan Rift/Wrench Basins and Passive Margins. Memóires du Muséum National d'Histoire Naturelle, vol. 186. Paris, pp. 607–627.

Geological Map of Syria. Scale 1:200 000, 1964.V. Ponikarov (Editor), TechnoExport, Moscow, Ministry of Industry of the S.A.R., Damascus.

Harmanşah, Ömür, 1999. Limestone hills of North Syria in late antiquity: problems of rural decline, final paper. Decline: All Good Things Must Come to an End? Second Graduate Symposium (October 15–16).

Harris, L.B., Koyi, H.A., Fossen, H., 2002. Mechanisms for folding of high-grade rocks in extensional tectonic settings. Earth Sci. Rev. 59, 163–210.

Karakhanyan, A.S., Balassanian, V.S., 1992. Aktivnaya dinamika zoni Spitakskogo zemletryaseniya 1988 [Active Dynamics of the 1988 Spitak Earthquake Zone]. Izvestiya AN Armenii. Nauki o Zemle, vol. 2, pp. 2–21 (in Russian).

Korjenkov, A., Mazor, E., 1999. Earthquake characteristics reconstructed from archaeological damage patterns: Shivta, the Negev Desert, Israel. Isr. J. Earth-Sci. 48, 265–282.

Korjenkov, A., Mazor, E., 2003. Archaeoseismology in Mamshit (southern Israel): cracking a millennia code of earthquakes preserved in ancient ruins. Archaeologischer Anzeiger 2, 51–82.

Korjenkov, A., Kaiser, D., 2002. Macroseismic Indications in Wittstock for a Historical Damaging Earthquake in Northern Germany. European Geophysical Society. (XXVII General Assembly Contact: This poster is available from: Nice, France, 21–26 April http://www.geo.unijena.de/geophysik/seismologie/egs02wittstock.pdf; Poster NH016).

Krenker, D., 1939. Die Wahlfahrtskirche des Simon Stylites in Kal'at Sim'an. Abhandlungen des Preussischen Akademie der Wissenschaften, vol. 4. Akademie-Verlag, Berlin.

Marco, S., Rockwell, T.K., Heimann, A., Frieslander, U., Agnon, A., 2005. Late Holocene activity of the Dead Sea Transform revealed in 3D palaeoseismic trenches on the Jordan Gorge segment. Earth Planet. Sci. Lett. 234, 189–205.

Meghraoui, M., Gomez, F., Sbeinati, R., van der Woerd, J., Mouty, M., Nasser Darkal, Abdul, Radwan, Y., Layyous, I., Al Naijar, H., Darawcheh, R., Hijazi, F., Al-Ghazzi, R., Barazandi, M., 2003. Evidence for 830 years of seismic quiescence from paleoseismology, archaeoseismicity and historical seismicity along the Dead Sea fault in Syria. Earth Planet. Sci. Lett. 210, 35–52.

Nelson, M.R., Jones, C.H., 1987. Palaeomagnetism and crustal rotations along a shear zone, Las Vegas Range, Southern Nevada. Tectonics 6, 13–33.

Nur, A., Cline, E.H., 2000. Poseidon's Horses: Plate Tectonics and Earthquake Storms in the Late Bronze Age Aegean and Eastern Mediterranean, Journal of Archaeological Science, 27, 43–63 Article No. jasc.1999.0431, available online at http://www.idealibrary.com.

Ponikarov, V.P., Kazmin, V.G., Mikhailov, I.A., Razvalyaev, A.V., Krasheninnikov, V.A., Kozlov, V.V., Soulidi-Kondratyev, E.D., Mikhailov, K.Ya., Kulakov, V.V., Faradjev, V.A., Mirzayev, K.M., 1967. Geological map of Syria, scale 1:500,000. Explanatory Notes. Part I: Ministry of Industry, Damascus (230 pp.).

Randall, D.E., Taylor, G.K., Grocott, J., 1996. Major crustal rotations in the Andean margin; palaeomagnetic results from the Coastal Cordillera of northern Chile. J. Geophys. Res. 101 (B7), 15783–15798.

Rappoport, P.A., 1994. Stroitelnoe proizvodstvo Drevnei Rusi (X–XIII vv). Glava 3: Organizacia stroitelxstva. Nauka, Moscow (SPB, 140 pp., in Russian).

Rukieh, M., Trifonov, V.G., Dodonov, A.E., Minini, H., Ammar, O., Ivanova, T.P., Zaza, T., Yusef, A., Al-Shara, M., Jobaili, Y., 2005. Neotectonic map of Syria and some aspects of Late Cenozoic evolution of the north-western boundary zone of the Arabian plate. J. Geodyn. 40, 235–256.

Sbeinati, M.R., Darawcheh, R., Mouty, M., 2005. The historical earthquakes of Syria: an analysis of large and moderate earthquakes from 1365 B.C. to 1900 A.D. Ann. Geophys. 48 (3), 347–435.

Syria, Archaeology from Space Atlas, 2002. General Organization of Remote Sensing (GORS). GEOSPACE-Verlag. (Damascus., 153 pp.).

Tatar, O., Piper, J.D.A., Gursoy, H., Heimann, A., Kocbulut, F., 2004. Neotectonic deformation in the transition zone between the Dead Sea Transform and the East Anatolian Fault Zone, Southern Turkey: a paleomagnetic study of the Karasu Rift volcanism. Tectonophysics 385, 17–43.

Tchalenko, G., 1953. Villages antiques de la Syrie du Nord. Part I, II. Volume L. Institut Français D'Archeology de Beyrouth, Bibilioteque Arceologique et Historique. Paris.

Westaway, R., 2004. Kinematic consistency between the Dead Sea Fault Zone and the Neogene and Quaternary left-lateral faulting in SE Turkey. Tectonophysics 391 (1–4), 203–237.

Yegian, M.K., Ghahraman, V.G., 1992. Damage statistics versus geologic and soil profiles. Report No. CE-92-11: The Armenia Earthquake of December 1988: Engineering and Reconstruction Aspects. Department of Civil Engineering, Northeastern University, Boston, Massachusetts, p. 02115 (190 pp.).